รายงานวิจัยฉบับสมบูรณ์

โครงการ การสลายตัวเชิงเร่งของน้ำมันทาร์จากแกซิฟิเคชันชีวมวลด้วยตัวเร่งปฏิกิริยาคาร์บอน

โดย ดร.สุภชิตา เกริกไกวัล
บัณฑิตวิทยาลัยร่วมด้านพลังงานและสิ่งแวดล้อม
มหาวิทยาลัยเทคโนโลยีพระจอมเกล้าธนบุรี

30 มิถุนายน 2561

สัญญาเลขที่ TRG5880183

รายงานวิจัยฉบับสมบูรณ์

โครงการ การสลายตัวเชิงเร่งของน้ำมันทาร์จากแกซิฟิเคชันชีวมวลด้วยตัวเร่งปฏิกิริยาคาร์บอน

ดร.สุภชิตา เกริกไกวัล
บัณฑิตวิทยาลัยร่วมด้านพลังงานและสิ่งแวดล้อม
มหาวิทยาลัยเทคโนโลยีพระจอมเกล้าธนบุรี

สนับสนุนโดยสำนักงานกองทุนสนับสนุนการวิจัยและ
มหาวิทยาลัยเทคโนโลยีพระจอมเกล้าธนบุรี

Abstract (บทคัดย่อ)

Project Code : TRG5880183
(รหัสโครงการ)

Project Title : Decomposition of biomass derived tar from gasification process by using carbon based catalysts
(ชื่อโครงการ) การสลายตัวเชิงเร่งของน้ำมันทาร์จากแกซิฟิเคชันชีวมวลด้วยตัวเร่งปฏิกิริยาคาร์บอน

Investigator : ดร.สุภชิตา เกริกไกวัล
บัณฑิตวิทยาลัยร่วมด้านพลังงานและสิ่งแวดล้อม
มหาวิทยาลัยเทคโนโลยีพระจอมเกล้าธนบุรี

E-mail Address : supachita.kre@kmutt.ac.th, supachita_k@hotmail.com

Project Period : 3 years 1st July 2015 to 30th June 2018
(including extended period 1 year)
(ระยะเวลาโครงการ) 3 ปี ระหว่าง วันที่ 1 กรกฎาคม 2558 ถึง 30 มิถุนายน 2561
(รวมระยะเวลาขยายโครงการ 1 ปี)

Abstract

Tar is the main technical concerns in biomass gasification process. Tar reduction is essential for the gas cleaning process. In this study, the catalytic tar decomposition using the carbon-based catalysts was investigated. Attractiveness of the carbon-based catalysts is a relatively low cost due to the simple preparation method that could be produced inside the gasifier. The carbon-based catalysts have also been reported as the effective catalyst for tar reduction. Effects of carbon-based catalyst preparation conditions such as steam activation, solvent treatment and the type of biomass on the catalyst properties as well as the catalytic for tar decomposition were studied. The study is divided into 3 parts; Part I Preparation of the various types of

carbon-based catalyst, Part II Catalytic decomposition of model tar compound and Part III Catalytic decomposition of biomass real tar.

In Part I, four types of carbon-based catalyst were prepared from the high potential biomass in Thailand including rice straw (RS), Napier grass (NP), sugarcane top/leaf (CTL) and palm empty fruit bunch (EFB). The catalysts or chars were prepared from the slow-heating pyrolysis at 800ºC for 30 min of holding time. From the BET analysis rice straw char had the highest BET surface area as high as 62.3 m^2/g. Hence, the rice straw char was choose as the carbon-based catalyst for the decomposition of tar in Part II and III. In Part II, naphthalene was selected as the model tar compound because it is the high thermal stable tar and it is the main chemical composition of the biomass tar. Rice straw char (RSC) was used as the reference carbon-based catalyst. Effects of char preparation including steam activation and solvent treatment on the catalytic performance in naphthalene decomposition were studied. Results revealed that the steam activated chars (SRS) showed the better catalytic activity than the RSC due to the enhancement of surface porosity. However, it was rapid deactivated by coking or tar deposition. In addition, the solvent treated char (ResC) gave the lower naphthalene conversion compared to the RSC but it provided the high H_2 and CH_4 productions. The catalytic mechanism of the ResC could describe by the existence of AAEMs on the char surface that may present as the stable form of alkali-silicate (i.e. K-Si). In port III, the rice straw (RS) and Luecaena wood (LN) were selected as the biomass samples. Catalytic effects of the char prepared from pure coal, pure biomass and the coal/biomass blends on tar conversion and gas production from tar steam reforming were investigated. Experiments were carried out in a two-stage fixed bed reactor that consisting of the devolatilization zone (volatile released zone) at the upper part and tar-char contacting zone at the lower-part. Effects of devolatilization temperature on tar chemical composition and catalytic performance were studied. Results showed that with the presence of catalyst, tar released at 700ºC could be the most efficiently decomposed to generate a highest gaseous products. Tar composition was the dominant effect on the degree of tar steam reforming. Comparing with biomass char, coal/biomass blended char showed the better catalytic performance both for RS and LN cases. This indicates the somewhat synergetic interactions between the blended char and the released tar. Catalytic mechanisms of each chars on tar reforming were also determined by the characterization of char before and after used. Outcome of this study

can be beneficial for the efficient tar removal process by using the low-cost carbon based catalysts in biomass gasification system.
Keywords : Tar cracking, tar steam reforming, carbon-based catalyst, gas production, coking
(คำหลัก) การสลายตัวของน้ำมันทาร์, รีฟอร์มมิ่งของน้ำมันทาร์, ตัวเร่งปฏิกิริยาคาร์บอน, ปฏิกิริยาการเกิดโค้ก

บทคัดย่อ

กระบวนการแกซิฟิเคชันชีวมวล (biomass gasification) เป็นหนึ่งในกระบวนการแปรรูปทางเคมีความร้อนที่มีประสิทธิภาพ โดยจะอาศัยหลักการเผาไหม้บางส่วน (partial oxidation) เพื่อให้ได้ผลิตภัณฑ์หลักเป็นแก๊สสังเคราะห์ (synthesis gas) ที่มีองค์ประกอบหลักคือ ไฮโดรเจน (H_2) และ คาร์บอนมอนอกไซด์ (CO) แก๊สสังเคราะห์สามารถนำไปใช้ประโยชน์ได้อย่างหลากหลาย ทั้งการนำไปเผาตรง (direct combustion) เพื่อให้พลังงานในการผลิตความร้อนและไฟฟ้า หรือนำไปใช้เป็นสารตั้งต้นในการผลิตสารปิโตรเคมีที่สำคัญ เช่น เมทานอล หรือน้ำมันเชื้อเพลิงเหลวสังเคราะห์ เป็นต้น จึงทำให้กระบวนการแกซิฟิเคชันมีความสำคัญและได้รับความสนใจอย่างมากในปัจจุบัน อย่างไรก็ตามปัญหาทางเทคนิคที่สำคัญอย่างหนึ่งของกระบวนการนี้ก็คือ น้ำมันทาร์ (Tar) ซึ่งจะมีมากเมื่อใช้ชีวมวลเป็นเชื้อเพลิง กระบวนการกำจัดน้ำมันทาร์ (tar removal process) จึงมีความจำเป็นอย่างมาก ก่อนนำแก๊สเชื้อเพลิงที่ผลิตได้ไปใช้งาน กระบวนการสลายตัวของทาร์เชิงเร่งปฏิกิริยา (catalytic tar cracking) เป็นหนึ่งในกระบวนการกำจัดทาร์ที่น่าสนใจ ซึ่งนอกจากจะสามารถลดปริมาณน้ำมันทาร์ลงได้แล้วส่วนหนึ่งยังสามารถเพิ่มปริมาณแก๊สผลิตภัณฑ์ได้ในเวลาเดียวกัน ตัวเร่งปฏิกิริยาที่นิยมใช้มากในกระบวนการสลายตัวของทาร์ ได้แก่ ตัวเร่งปฏิกิริยากลุ่มโลหะ เช่น ตัวเร่งปฏิกิริยานิกเกิล (Ni-based catalyst) หรือตัวเร่งปฏิกิริยากลุ่มเหล็ก (Fe-based catalysts) ตัวเร่งปฏิกิริยากลุ่มนี้มีประสิทธิภาพในการสลายตัวของน้ำมันทาร์ได้ค่อนข้างสูง และยังสามารถกำหนดการเลือกเกิดของผลิตภัณฑ์แก๊ส (selectivity) ได้จากการออกแบบตัวเร่งปฏิกิริยาที่เหมาะสม อย่างไรก็ตามข้อจำกัดของตัวเร่งปฏิกิริยาโลหะ ก็คือ ราคาแพง มีขั้นตอนในการเตรียมซับซ้อน และเกิดการเสื่อมสภาพ (deactivation) ได้ง่าย เนื่องจากการเกิด coke deposition และจากการเกิดการหลอมรวมตัวกัน (sintering) ระหว่างโลหะ ดังนั้น ในการศึกษานี้ สนใจที่จะศึกษาตัวเร่งปฏิกิริยาฐานคาร์บอน (carbon-based catalyst) ซึ่งมีข้อดีคือ มีราคาถูก เตรียมได้ง่าย และสามารถเตรียมได้ภายในเตาผลิตแก๊สจากการปรับภาวะดำเนินการ นอกจากนี้ ตัวเร่งปฏิกิริยาฐานคาร์บอน มีคุณสมบัติที่เป็นรูพรุนและมีองค์ประกอบอัลคาไลและอัลคาไลน์เอิทธ์ (AAEMs) ซึ่งเชื่อว่าจะสามารถมีประสิทธิภาพในการเร่งการสลายตัวของน้ำมันทาร์ได้ โดยตัวเร่งปฏิกิริยาฐานคาร์บอน จะถูกเตรียมขึ้นจากกระบวนการไพโรไลซิสของถ่านหิน ชีวมวล และถ่านหินผสมชีวมวล เพื่อนำมาทดสอบใช้ในการเป็นตัวเร่งปฏิกิริยาของการสลายตัวน้ำมันทาร์ต่อไป โดย

การศึกษานี้ แบ่งการทดลองออกเป็น 3 ส่วน ดังนี้ ส่วนที่ 1 การเตรียมตัวเร่งปฏิกิริยาฐานคาร์บอน ส่วนที่ 2 การศึกษาผลเชิงเร่งปฏิกิริยาของตัวเร่งปฏิกิริยาฐานคาร์บอนต่อการสลายตัวของแบบจำลองน้ำมันทาร์ และส่วนที่ 3 การศึกษาผลเชิงเร่งปฏิกิริยาของตัวเร่งปฏิกิริยาฐานคาร์บอนต่อการสลายตัวของน้ำมันทาร์จากชีวมวลจริง

จากการศึกษาในส่วนที่ 1 ได้มีการเตรียมตัวเร่งปฏิกิริยาจากชีวมวล 4 ชนิด ที่มีศักยภาพสูงในประเทศไทย ได้แก่ ฟางข้าว หญ้าเนเปียร์ ใบและยอดอ้อย และทะลายปาล์มเปล่า โดยเตรียมด้วยกระบวนการไพโรไลซิสแบบช้า ที่ 800 องศาเซลเซียส holding time 30 นาที พบว่า ไพโรไลซิสชาร์ที่ได้จากฟางข้าว มีค่าพื้นที่ผิว BET สูงที่สุด คือ 62.3 ตารางเมตรต่อกรัม ในขณะที่ ไพโรไลซิสชาร์จากหญ้าเนเปียร์, ใบและยอดอ้อยและทะลายปาล์มเปล่า มีค่าพื้นที่ผิว BET ค่อนข้างต่ำ คือ 4.8, 29.4 และ 3.9 ตารางเมตรต่อกรัม ตามลำดับ เนื่องจากพื้นที่ผิวเป็นปัจจัยสำคัญต่อการเร่งปฏิกิริยาการสลายตัวของน้ำมันทาร์ ดังนั้นในการทดลองส่วนถัดไป จึงเลือกใช้ไพโรไลซิสชาร์จากฟางข้าวเป็นตัวเร่งปฏิกิริยาฐานคาร์บอน โดยการศึกษาส่วนที่ 2 มุ่งศึกษาการสลายตัวของแบบจำลองของทาร์ ในที่นี้ เลือกใช้ แนฟทาลีน (Naphthalene) เนื่องจากเป็นองค์ประกอบส่วนใหญ่ของทาร์จากชีวมวลและมีเสถียรภาพทางความร้อนสูง โดยเลือกตัวเร่งปฏิกิริยาฐานคาร์บอนที่เตรียมจากไพโรไลซิสฟางข้าว (RSC) นอกจากนี้ได้ทำการศึกษาผลของการเตรียมตัวเร่งปฏิกิริยาจากฟางข้าว โดยศึกษาผลของการกระตุ้นชาร์ด้วยไอน้ำ (steam activation) และการทรีทเมนต์ด้วยตัวทำละลาย (solvent treatment) ต่อสมบัติของถ่านชาร์ และต่อประสิทธิภาพการเร่งปฏิกิริยาของถ่านชาร์สำหรับการสลายตัวของแนฟทาลีนด้วย จากผลการศึกษา พบว่า ตัวเร่งปฏิกิริยาชาร์จากฟางข้าวที่ผ่านการกระตุ้นด้วยไอน้ำที่อุณหภูมิสูง (SRS800) จะทำให้ค่าร้อยละการเปลี่ยนแนฟทาลีน (naphthalene conversion, %) เพิ่มสูงขึ้น ในขณะเดียวกันก็ให้ผลิตภัณฑ์แก๊สสูงขึ้นด้วย โดยกลไกหลักที่ทำให้ตัวเร่ง SRS800 มีประสิทธิภาพเชิงเร่งปฏิกิริยาสูง ก็คือ การเพิ่มขึ้นของพื้นที่ผิว BET มากกว่า 3 เท่า เมื่อเทียบกับตัวเร่งปฏิกิริยาก่อนการกระตุ้นด้วยไอน้ำ อย่างไรก็ตาม พบว่าตัวเร่งปฏิกิริยาที่ผ่านการกระตุ้นด้วยไอน้ำเกิดการเสื่อมสภาพจากการเกิด coke deposition ได้เร็วกว่าตัวเร่งปฏิกิริยาก่อนการกระตุ้น นอกจากนี้ยังพบว่า ในกรณีของตัวเร่งปฏิกิริยาที่ผ่านกระบวนการทรีทเมนต์ด้วยตัวทำละลาย (ResC) จะให้ค่าร้อยละการเปลี่ยนของแนฟทาลีนต่ำกว่าตัวเร่งปฏิกิริยาก่อนการทรีทเมนต์ แต่จะให้ค่าแก๊สผลิตภัณฑ์สูงกว่า โดยเฉพาะอย่างยิ่งไฮโดรเจน (H_2) และ มีเทน (CH_4) ทั้งนี้เนื่องมาจากการมีอยู่ขององค์ประกอบอัลคาไลและอัลคาไลน์เอิทธิ์ในรูปของซิลิเกต ซึ่งเป็นองค์ประกอบที่เสถียร และสามารถทำหน้าที่เร่งการเกิดปฏิกิริยาการสลายตัวของแนฟทาลีนได้นั่นเอง จากการศึกษาสมบัติของตัวเร่งปฏิกิริยาก่อนและหลังใช้ในการสลายตัวของแนฟทาลีนทำให้สามารถกำหนดกลไกการเกิดปฏิกิริยาของตัวเร่งปฏิกิริยาแต่ละชนิดได้

การศึกษาส่วนที่ 3 เป็นการนำตัวเร่งปฏิกิริยาฐานคาร์บอนมาใช้ในการเร่งปฏิกิริยาการสลายตัวของน้ำมันทาร์ที่เกิดจากชีวมวลจริง โดยจะศึกษาถึงชนิดของตัวเร่งปฏิกิริยาและอุณหภูมิในขั้นปลดปล่อยไอระเหย (devolatilization temperature) ของชีวมวลที่มีต่อ

ประสิทธิภาพการเร่งปฏิกิริยา โดยการทดลองจะทำในเตาปฏิกรณ์เบดนิ่งสองขั้นตอน ตัวเร่งปฏิกิริยาเตรียมจาก กระบวนการไพโรไลซิสของถ่านหิน, ชีวมวล (ฟางข้าวและไม้กระถิน) และจากการไพโรไลซิสร่วมของถ่านหินและชีวมวล (co-pyrolysis) จากการศึกษาพบว่า ตัวเร่งปฏิกิริยาที่เตรียมจากการไพโรไลซิสร่วม (co-pyrolysis char) มีประสิทธิภาพเชิงเร่งปฏิกิริยาสูงกว่าชาร์ของชีวมวลเดี่ยว และเทียบเคียงกับถ่านชาร์จากถ่านหิน (coal char) ทั้งนี้เนื่องจากการเกิดอันตรกิริยาเชิงบวก (synergy effect) ระหว่างถ่านหินและชีวมวล ซึ่งเกิดขึ้นระหว่างกระบวนการไพโรไลซิสร่วม ส่งผลให้ชาร์ที่ได้มีค่าพื้นที่ผิวหรือความเป็นรูพรุนสูงขึ้น นอกจากนี้ยังพบว่า ตัวเร่งปฏิกิริยาจะสามารถสลายตัวน้ำมันทาร์ที่ปลดปล่อยที่อุณหภูมิการปลดปล่อยไอระเหยที่ 700 องศาเซลเซียส ได้ดีกว่าการสลายตัวน้ำมันทาร์ที่ปลดปล่อยที่อุณหภูมิ 600 และ 800 องศาเซลเซียส ซึ่งแสดงให้เห็นว่าองค์ประกอบของน้ำมันทาร์มีผลอย่างมากต่อประสิทธิภาพเชิงเร่งปฏิกิริยาของตัวเร่งปฏิกิริยาฐานคาร์บอน ผลจากการศึกษานี้ สามารถนำไปต่อยอดและประยุกต์ใช้ในการออกแบบกระบวนการผลิตแก๊สจากชีวมวล (biomass gasification) ที่มีการนำตัวเร่งปฏิกิริยาฐานคาร์บอนซึ่งมีราคาถูก (low-cost carbon-based catalyst) ได้อย่างมีประสิทธิภาพ

Executive Summary

Tar is the main technical concerns in biomass gasification process. It is the condensable hydrocarbons that can plug or block the process equipment and lowering the overall process efficiency. Therefore, tar removal process is necessary. This study, catalytic tar cracking using the carbon-based catalyst was proposed to remove the tar together with increase the gas products. Attractiveness of the carbon-based catalysts is a relatively low cost because of the easy preparation that could be produced inside the gasifier. They have also been reported as the effective catalyst for tar reduction. Effects of carbon-based catalyst preparation conditions such as steam activation, solvent treatment and the type of biomass on the catalyst properties as well as the catalytic for tar decomposition were investigated. The study is divided into 3 parts; Part I Carbon-based catalyst preparation, Part II Catalytic decomposition of model tar compound and Part III Catalytic decomposition of biomass real tar.

In part I, four types of carbon-based catalyst were prepared from the high potential biomass in Thailand including rice straw, Napier grass, sugarcane top/leaf and palm empty fruit bunch. The catalysts or chars were prepared from the slow-heating pyrolysis at 800ºC for 30 min of holding time. From the BET analysis rice straw char had the highest BET surface area as high as 62.3 m^2/g. While, the Napier grass char, sugarcane top/leaf char and EFB char had the lower in BET surface area of 4.8, 29.4

and 3.9 m^2/g, respectively. Hence, the rice straw char was selected as the carbon-based catalyst for the decomposition of tar in Part II and III.

In part II, naphthalene was selected as the model tar compound because it is the most stable tar and it is the main chemical composition of the biomass tar. Rice straw char (RSC) was used as the reference carbon-based catalyst. Effects of char preparation including steam activation and solvent treatment on the catalytic performance in naphthalene decomposition were studied. Results revealed that the steam activated chars (SRS) showed the better catalytic activity than the RSC due to the enhancement of surface porosity that increasing about 3-times compared to the RSC. However, the SRS catalyst was rapid deactivated by coking or tar deposition. In addition, the solvent treated char (ResC) gave the lower naphthalene conversion compared to the RSC but it provided the high H_2 and CH_4 productions. The catalytic mechanism of the ResC could describe by the existence of AAEMs on the char surface that may presented as in the stable form of alkali-silicate (i.e. K-Si). The existence of AAEMs could promote the naphthalene decomposition in the vapor phase. However, the rate of deactivation by tar deposition on the porosity of ResC was faster than the catalytic activity of AAEM therefore the ResC showed the lower catalytic performance than the RSC.

In port III, the rice straw (RS) and Luecaena wood (LN) were selected as the biomass samples. Catalytic effects of the char prepared from pure coal, pure biomass and the coal/biomass blending on tar conversion and gas production from tar cracking and tar steam reforming were investigated. Experiments were carried out in a two-stage fixed bed reactor that consisting of the devolatilization zone (volatile released zone) at the upper part and tar-char contacting zone at the lower-part. Effects of devolatilization temperature on tar chemical composition and catalytic performance were studied. Results showed that with the presence of catalyst, tar released at 700ºC could be the most efficiently decomposed to generate a highest gaseous products. Tar composition was the dominant effect on the degree of tar cracking as well as tar reforming. Comparing with biomass char, coal/biomass blended char showed the better catalytic performance both for RS and LN cases. This indicates the somewhat synergetic interactions between the blended char and the released tar. Catalytic mechanisms of each chars on tar reforming were also determined by the characterization of char before and after used. Outcome of this study can be beneficial for the efficient tar removal process by using the low-cost carbon based catalysts in biomass gasification system.

Research Content (เนื้อหาวิจัย)

1. Objective and Scopes

Objectives of this research are listed below

1) To prepare and characterized the carbon-based catalysts from the various types of coal and biomass in Thailand which are expected to be a catalyst for tar decomposition.

2) To investigate the catalytic effect of the prepared carbon-based catalysts on biomass derived tar decomposition

This research is divided into 3 parts including;

Part 1: Carbon-based catalyst preparation

In this part, the various type of carbon-based catalysts were prepared from four types of biomass which has high potential in Thailand i.e. rice straw (RS), Napier grass (NP), sugarcane top/leaf (CTL) and empty fruit bunch (EFB). Surface properties of the catalysts were measured by the Brunauer-Emmet-Teller (BET) analyser. Morphology and element composition of the char were analyzed by Scanning Electron Microscopy (SEM) equipped with Energy Dispersive Spectroscopy (EDS). From the characterization, the catalyst which has the highest BET surface area would be selected to apply as the catalyst for the decomposition of tar in Part II and Part III.

Part 2: Catalytic performance of the carbon-based catalyst on the decomposition of model tar compound

In this part, the rice straw char was selected as the carbon-based catalyst for the decomposition of model tar compound. Naphthalene was choose as the model tar compound due to its high thermal stability. Effects of char preparation condition i.e. steam activation and solvent treatment on the char properties and the catalytic performance on tar cracking were investigated. Catalytic mechanism of each catalyst for naphthalene decomposition was also proposed.

Part 3: Catalytic performance of the carbon-based catalyst on the decomposition of biomass derived tar

In this prat, the decomposition of real biomass derived tar steam reforming was studied. The chars was prepared from rice straw (RS) and Leucaena wood (LN) to apply as the catalyst for tar steam reforming of raw biomass. Effect of devolatilization temperature (at tar release zone) on the tar composition and the tar decomposition was investigated.

2. Details of Part 1: Carbon-based catalyst preparation

2.1 Material and Method

2.1.1 Materials

Four types of the high potential biomass in Thailand i.e. rice straw (RS), Napier grass (NP), sugarcane top/leaf (CTL) and empty fruit bunch (EFB) were selected. Proximate and ultimate analyses of the biomass sample is shown in Table 1. It was found that the moisture content of all biomass was about 8 – 10 wt%. Ash content was varied from 2 – 17 wt%. CTL has the lowest ash content while RS contains the highest ash content. Fixed carbon (FC) is the one major factor to determine the char yield. It was found that RS has the highest FC approximately 14 wt%, while the EFB has the lowest FC. From ultimate analysis and HHV, 2 groups of biomass can be divided RS and NP had the low C and high O contents resulting in the lower HHV when comparing with the group of EFB and CTL. These results will be related to the char yields of each biomass which are presented in Table 2 that would discuss in the next section.

Table 1 Proximate and Ultimate analysis of raw materials

Fuel sample	Rice straw (RS)	Napier grass (NP)	Palm empty fruit bunch (EFB)	Sugar cane Top/Leave (CTL)
Moisture (wt% as received)	10.2	9.5	9.5	8.7
Proximate analysis (wt%, dry basis)				
Ash	16.9	8.9	7.8	2.3
Volatile matter	68.7	80.9	83.8	88.2
Fixed carbon	14.3	10.0	8.3	9.4
Ultimate analysis (wt%, daf basis)				
Nitrogen (N)	1.2	3.1	0.6	2.2
Carbon (C)	37.9	38.1	50.9	51.6
Hydrogen (H)	4.8	5.0	7.1	4.1
Oxygen (O)	55.7	53.7	41.3	41.9
High heating value (HHV, MJ/kg dry)	15.3	15.6	17.2	16.1

2.1.2 Char preparation

Biomass sample was ground and sieved into the particle size of 150 - 250 μm and dried at 110ºC for at least 12 hours before the catalyst preparation process. Slow pyrolysis and steam activation experiments of biomass were conducted in a horizontal fixed bed reactor as illustrated in Fig. 1. The reactor consists of an electric furnace, a quartz tube reactor (38 mm-I.D. and 70 cm-length) and steam generator unit. About 3 grams of dried biomass was placed in a quartz boat which was located at the middle of the heating zone. The reactor was purged with N_2 at the flow rate of 100 mL/min for 1.5 hour to remove oxygen in the system. After purging, the electric furnace was heated to 800ºC with heating rate of 10ºC/min and 30 minutes of holding time and then naturally cool down to room temperature. The pyrolysis char was weighed and kept in the desiccator before use.

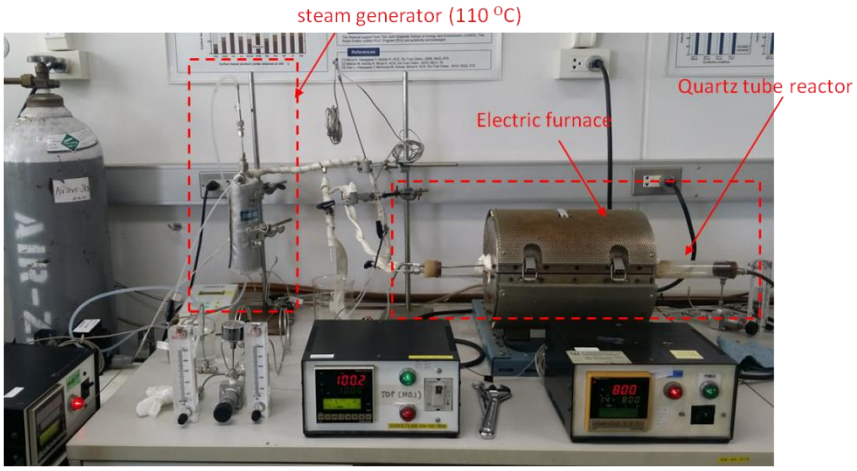

Fig.1 A horizontal lab-scaled fixed bed reactor for biochar preparation

To increase the BET surface area of the char, the steam activation was applied in this part. About 1 gram of pyrolysis char was used for the steam activation experiment. After purging with N_2 for 1.5 hr, the electric furnace was heated up to 800ºC with heating rate of 10ºC/min. As soon as the set temperature was reached, 50% (v/v) of steam/N_2 mixture with a total flow rate of 100 mL/min was introduced into the reactor for 30 min of steam exposing time.

2.2 Result and discussion

Char yields after slow pyrolysis and after steam activation are presented in Table 2. It was found that after pyrolysis at 800ºC, rice straw gave the highest char yield approximately 34 wt%. This corresponds to the highest fixed carbon of rice straw. In contrast, NP, EFB and CTL had the lower char yields due to the relatively lower fixed carbon compared to RS. After steam activation, rice straw char also provide the highest char yield about 22 wt% basis the raw rice straw. It means that only 32% weight of rice

straw char was loss during the steam activation. While, the other chars (NP, CTL and EFB) the yield of char after steam activation were lower, in particular EFB. It was found that EFB char after steam activation yields only 7 wt% of raw EFB sample. In the viewpoint of char or catalyst yield, the rice straw char was choose as the carbon-based catalyst for the study in Part II and III.

Table 2 Char yield from the pyrolysis of biomass

Pyrolysis Char	Char yield after pyrolysis (wt%)	Char yield after activation (wt% of raw biomass)
Rice straw (RS)	34.1	22.0
Empty fruit bunch (EFB)	27.8	7.1
Napier grass (NP)	29.8	17.6
Sugarcane Top/Leaf (CTL)	25.6	14.6

Moreover, the surface properties of the prepared chars including surface area, total pore volume and average pore diameter were measured by using the BET analyzer. The result is shown in Table 3. It was found that after pyrolysis, the rice straw char had the highest BET surface area and total pore volume but the pore diameter was quite small. BET surface area is the one of important factors to determine the catalytic performance of the char for tar reduction. Hence, in this study, the rice straw char was selected as the catalyst for tar reduction in Part II and part III.

Consider the surface properties of the char after steam activation, the BET surface area and total pore volume were extremely higher but the average pore diameter was smaller comparing with the pyrolysis char. This result indicates the promotion of carbon-steam reaction at high temperature resulting in the higher BET surface area and pore volume. One evidence can be proven by the SEM images of the char before and after steam activation as presented in Fig.2., example of NP and CTL cases. It can be clearly seen the higher porosity on the surface of the char after steam activation that occurring for all cases of the chars. Even though NP and CTL showed the relatively high BET surface area after steam activation, the char yield was quite small. Therefore, NP and CTL chars were not selected for the carbon-based catalyst in the next parts. Alternatively, rice straw char had the high yield as well as the high BET surface area, the rice straw char was selected as the carbon-based catalyst for the next parts.

Table 3 Surface properties of the prepared chars from the various type of biomass

Pyrolysis char	BET surface area (m^2/g)	Total pore volume (cm^3/g)	Average pore diameter (nm)
Rice straw (RS)	62.3	0.0589	3.78
Empty fruit bunch (EFB)	3.9	0.0135	16.47
Napier grass (NP)	4.7	0.0179	23.34
Sugarcane Top/Leaf (CTL)	29.4	0.0274	3.74
Activated char	BET surface area (m^2/g)	Total pore volume (cm^3/g)	Average pore diameter (nm)
Rice straw (RS)	341.1	0.215	2.52
Empty fruit bunch (EFB)	24.7	0.0649	10.49
Napier grass (NP)	504.6	0.316	2.52
Sugarcane Top/Leaf (CTL)	460.5	0.310	2.69

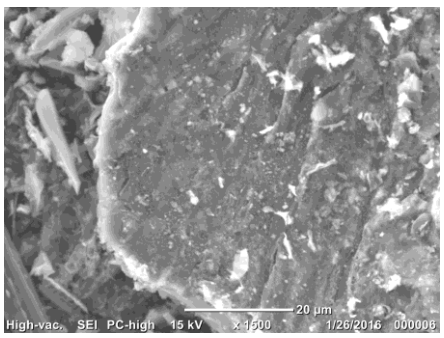

(a) NP char before activation

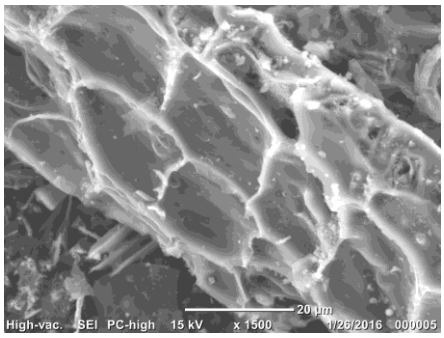

(b) NP char after activation

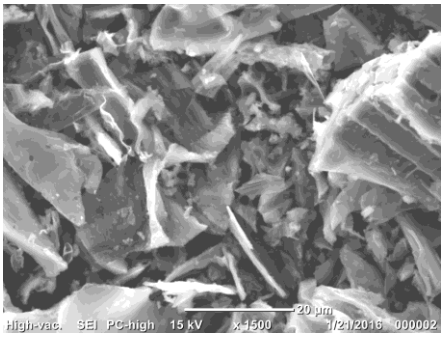

(c) CTL char before activation

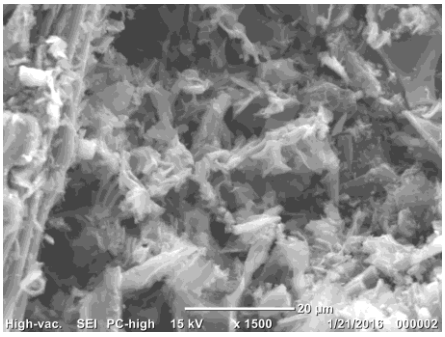

(b) CTL char after activation

Figure 2 SEM images of NP and CTL chars (magnification 1500X) before and after steam activation at 800ºC

3. Details of Part 2: Catalytic performance of the carbon-based catalyst on the decomposition of model tar compound

3.1 Material and Method

3.1.1 Model tar compound

In this section, naphthalene was selected as the model tar compound. From the previous report [1], at cracking temperature 800ºC, main composition of biomass derived tar is a polyaromatic hydrocarbon (PAH), as shown in Fig. 3. Naphthalene is the one of PAHs that could release from the biomass pyrolysis as well as the steam gasification of biomass [2]. It was also reported as the most stable tar that has the difficulty to decompose.

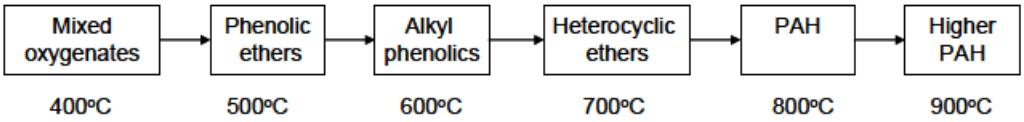

Figure 3 Tar maturation scheme [1]

3.1.2 Carbon-based catalyst preparation

Four types of carbon-based catalysts were prepared from rice straw. Rice straw was ground and sieved into the particle size of 150 - 250 μm and dried at 110ºC for at least 12 hours before the catalyst preparation process. Slow pyrolysis and steam activation experiments of rice straw were conducted in a horizontal fixed bed reactor as illustrated in Fig. 1. The reactor consists of an electric furnace, a quartz tube reactor (38 mm-I.D. and 70 cm-length) and steam generator unit. Details of pyrolysis of rice straw was previously described in Part I. The rice straw pyrolysis char, hereafter called “RSC” was weighed and kept in the desiccator before use. For steam activation experiment, about 1 gram of RSC was used. After purging with N2 for 1.5 hr, the electric furnace was heated up to the desired temperature (500 or 800ºC) with heating rate of 10ºC/min. As soon as the set temperature was reached, 50% (v/v) of steam/N_2 mixture with a total flow rate of 100 mL/min was introduced into the reactor for 30 min of steam exposing time. The steam activated RSC at 500ºC and 800ºC was called as “SRS500” and “SRS800”, respectively. Another catalyst was a rice straw residue char, hereafter called as “ResC”. The rice straw residue was an unextractable fraction derived from the degradative solvent extraction of rice straw which was conducted in an autoclave reactor using 1-methyl naphthalene as the solvent. The extraction was performed at 350ºC, final pressure around 4.5 bar and rice straw to solvent ratio of 1:20 (g:mL).

Detail of degradative solvent extraction procedure was reported elsewhere [3]. In this study, the rice straw residue was selected to be a source of carbon-based catalyst due to its relatively high mineral content. However, to increase surface area of the rice straw residue, a slow pyrolysis of residue was also conducted in the same manner with the pyrolysis of rice straw as described above. Nomenclature of the carbon-based catalysts and preparation condition are summarized in Table 4.

Table 4 Nomenclature of the prepared carbon-based catalyst and conditions

Char	Nomenclature	Condition
rice straw pyrolysis char	RSC	pyrolysis at 800 ^{O}C, holding time 30 min.
steam activated rice straw char at 500 ^{O}C	SRS500	expose the steam for RSC at 500 ^{O}C, exposing time 30 min.
steam activated rice straw char at 800 ^{O}C	SRS800	expose the steam for RSC at 500 ^{O}C, exposing time 30 min.
residue pyrolysis char	ResC	pyrolysis of Res at 800 ^{O}C, holding time 30 min.

3.1.3 Characterization of the carbon-based catalyst

The fresh carbon-based catalysts and the used catalysts after naphthalene decomposition were characterized by following techniques. Proximate analysis was conducted following ASTM D5172 using a thermogravimetric analyzer (TGA, Shimadzu model TA50) to give volatile matter, fixed carbon and ash content. Ultimate analysis was conducted by using the organic elemental micro analyzer (MICRO CORDER model JM10) to determine the contents of carbon, hydrogen and nitrogen while the content of oxygen was calculated by difference. The surface properties of the catalyst were characterized by Brunauer-Emmet-Teller analyzer (BET, model BELSORP-mini, BEL Japan, Inc.). The specific surface area and total pore volume of catalysts were determined from the corresponding nitrogen adsorption – desorption isotherms obtained at -196°C. Prior to the measurements, the samples were pretreated by heating up to 150°C and hold for 6 hours under vacuum. The surface area was measured by the Brunauer-Emmet-Teller (BET) calculation method applied to the adsorption branch of the isotherms. The total pore volume was defined as the volume of liquid nitrogen corresponding to the amount adsorbed at a relative pressure P/P_0 = 0.99.

In addition, functional groups of the fresh catalysts were qualitatively identified using a Fourier transform infrared (FTIR) spectrometer (JEOL, JIR-WINSPEC 50). FTIR spectra were acquired at 4 cm^{-1} resolution by averaging 32 scans in the range of 4000 to 400 cm^{-1} using a few milligrams of neat sample in a KBr disk. Morphology of the catalyst and elemental dispersion on the catalyst surface were also determined by the Scanning Electron Microscopy (SEM) equipped with Energy Dispersive Spectroscopy (EDS) (JEOL model JCM-6000).

Figure 4 Thermogravimetric analyzer (TGA, Shimadzu TA50) for proximate analysis

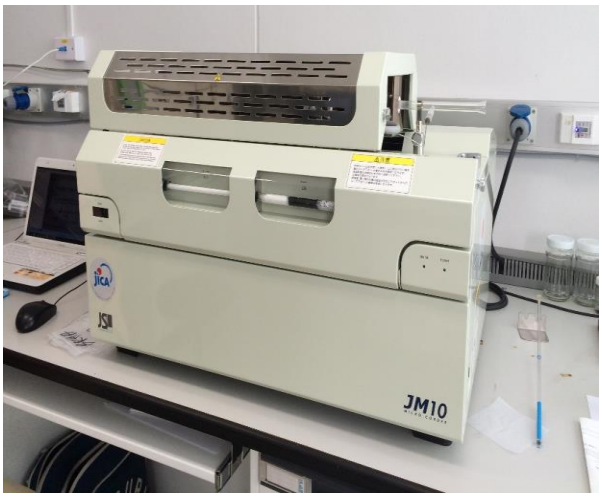

Figure 5 Organic elemental analyzer (OEA, MICRO CORDER JM10) for ultimate analysis

Figure 6 Brunauer-Emmet-Teller analyzer (BET, BELSORP-mini, BEL Japan, Inc.)

Figure 7 Fourier transform infrared (FTIR) spectrometer (JEOL, JIR-WINSPEC 50)

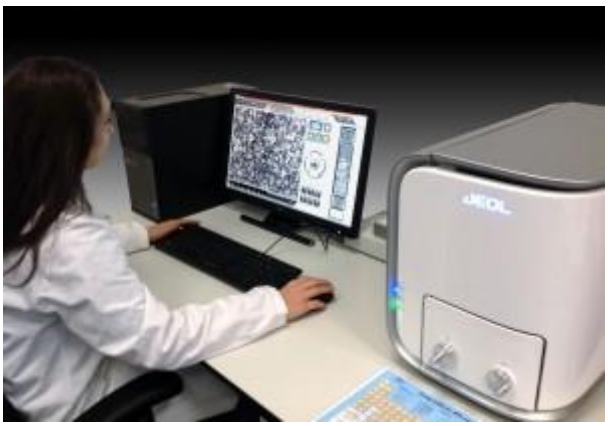

Figure 8 Scanning Electron Microscopy (SEM) equipped with Energy Dispersive Spectroscopy (EDS) (JEOL model JCM-6000) (https://blog.nikonmetrology.com)

3.1.4 Naphthalene Decomposition

Naphthalene decomposition was carried out in a lab-scale fixed bed reactor as shown in Fig. 9. The reactor consists of three main parts including naphthalene evaporator, reaction part and tar and gas collection part. At reaction part, a quartz reactor (460 mm-length and 10-mm I.D.) was set in a vertical electric furnace.

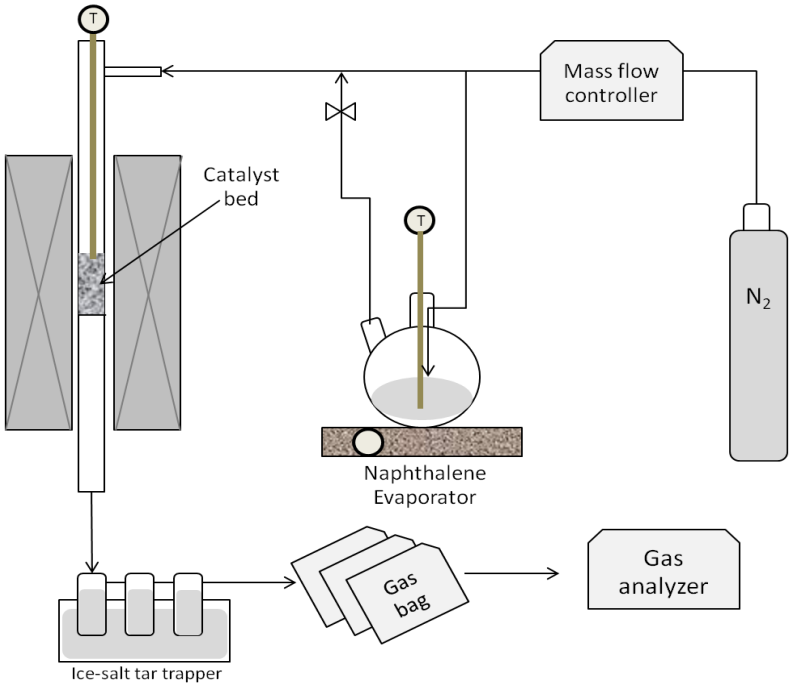

Figure 9 Schematic diagram of a lab-scale fixed bed reactor for naphthalene decomposition

About 0.30 g of a carbon-based catalyst (approximately 3 cm of bed height) was placed inside the reactor where the position of the reactor is at the middle of heating zone. Temperature inside the reactor was also measured by a K-type thermocouple which was placed on the surface of catalyst bed. Nitrogen with total flow rate of 100 mL min-1 was purged through the reactor (30 mL min-1) and the naphthalene evaporator (70 mL min-1) for 1.5 hour before testing to limit the oxygen concentration inside the system. The gas residence time over the catalyst bed was about 0.9 s. At naphthalene evaporator, about 3 g of solid naphthalene (99.0% purity, Himedia) was put inside the 250 mL round-bottom flask. Other connection parts, which that tar and naphthalene passed through, were also externally heated by heating tape (temperature set at 150ºC) to prevent the condensation of tar. For tar collection, a series of three impinge bottles filled with isopropanol were used. The impinge bottles were put in an ice-mix-salt cooling bath at temperature around -15 ºC. In each experiment, after purging with nitrogen, the reactor was heated to 800ºC, while the naphthalene flask was heated by

heating mantle and temperature inside was controlled around 120 - 130ºC to ensure that naphthalene was completely sublimated and presented as naphthalene vapor. When the reaction temperature was reached, the naphthalene vapor was allowed to pass into the reactor with a feed rate at 0.013 ± 0.002 g min-1 for 100 min of feeding time. In order to study the effect of catalyst on naphthalene decomposition, thermal cracking of naphthalene was also conducted by using inactive alumina balls (O.D. 3 mm.) with the same bed height instead of the catalyst bed. During naphthalene feeding, gas product was collected in 2-L gas bag every 20 min until the experiment stop.

Gas product was further characterized to examine main gas composition i.e. H_2, CH_4, CO and CO_2 by using GC-TCD/FID equipped with MS5A and Porapak Q columns (Shimadzu, GC-2014).

Figure 10 GC-TCD/FID (Shimadzu, GC-2014) for gas product analysis

Due to the decomposition of carbon-based catalyst at cracking temperature, the “blank” experiment was conducted to determine the gas generated from the catalyst itself. Note that the gas product presented in this study refers to the net gas after subtracting the gas from blank experiment. The condensable tar product, which was trapped in the tar trapper unit, was sampled to analyze the content of naphthalene by using GC-FID equipped with HP5/MS column (Shimadzu, GC2010). The naphthalene conversion can be calculated by the Eq. (1),

$$X = \frac{M_{in} - M_{out}}{M_{in}} \times 100 \qquad (1)$$

when X is naphthalene conversion (%), M_{in} is amount of naphthalene inlet calculating from the weight difference between naphthalene inside the round-bottom flask before and after experiment and M_{out} is amount of unreacted naphthalene (g) after experiment determining by the GC-FID.

3.2 Result and discussion

3.2.1 Characterization of the prepared char

3.2.1.1 Effect of steam activation on the char properties

Physical properties of the prepared chars are shown in Table 5. Consider the mass yield on the basis of raw rice straw, SRS500 had the slightly lower in mass yield while the SRS800 had about 30% lower in mass yield when comparing with RSC. It indicates that steam activation at higher temperature would largely promote the carbon-steam reaction resulting in the relatively low of char yield. In addition, from ultimate analysis, the SRS800 had the significantly lower in carbon content but higher in oxygen content when comparing with RSC as well as SRS500. It refers that the steam activation at high temperature could promote the carbon-steam reaction resulting in the loss of carbon content of the char and increase the proportion of oxy-functional groups on the carbon surfaces such as carbonyl (C=O) and carboxylic (-COOH) [4].

Table 5 Physical properties of the prepared char

	RSC	**SRS500**	**SRS800**	**ResC**
Mass yield				
(wt% of raw rice straw)	33.8	31.3	24.8	15.7
Proximate analysis				
(% dry basis)				
volatile matter	12.5	14.6	12.7	19.6
Fixed Carbon	37.4	43.1	36.1	12.5
Ash	50.1	42.3	51.2	67.9
Elemental analysis (wt% daf.)				
Carbon (C)	75.6	71.8	57.8	68.6
Hydrogen (H)	2.0	2.1	2.0	2.2
Nitrogen (N)	1.0	0.8	0.8	0.7
Oxygen (O)* by diff.	21.3	25.3	39.5	28.5
O/C molar ratio	0.21	0.26	0.51	0.31
AAEM analysis (wt% dry char)*				
Potassium (K)	6.40 ± 0.84	3.57 ± 1.04	4.41 ± 1.22	6.94 ± 1.41
Magnesium (Mg)	1.13 ± 0.11	0.52 ± 0.10	0.74 ± 0.08	0.73 ± 0.19
Calcium (Ca)	3.20 ± 0.08	0.35 ± 0.24	0.62 ± 0.07	1.30 ± 0.73
Silicon (Si)	5.57 ±1.01	16.88 ± 1.75	17.78 ± 2.89	13.44 ± 1.65

* by SEM-EDS determine by the average of selected area-specific data points

This result confirms by the FTIR spectra as shown in Fig. 11. It can be seen that for SRS800 (Fig. 11(c)), the peak of conjugated aromatic carbonyl/carboxyl C=O (band peak 1720 – 1690 cm^{-1}) was observed with a relatively high intensity. It was also observed in other chars but with low peak intensity. Moreover, from FTIR, it can be observed the band of aromatic ring stretching of C=C groups (peak at 1592 cm^{-1}) that presented in all chars. This result probably implies that all chars had the macromolecular structure of aromatic hydrocarbons. Consider the AAEM analysis on the basis of dry char sample, the SRS chars (both SRS500 and SRS800) had the lower in K, Mg and Ca contents compared to those of RSC but higher in Si content. It might be the effect of re-thermal treatment with the presence of steam under high temperature that could promote the volatilization of AAEMs, especially the AAEM-bonded with carbon in the char i.e. K-O-C [5, 6]. SRS500 and SRS800 had the comparable AAEM and Si contents. It means that the temperature during steam activation had a slightly effect on the content of AAEM on the char surface. Hence, the AAEMs, in particular K, in the SRS char would exist as the K-Si stable form which was different with the RSC.

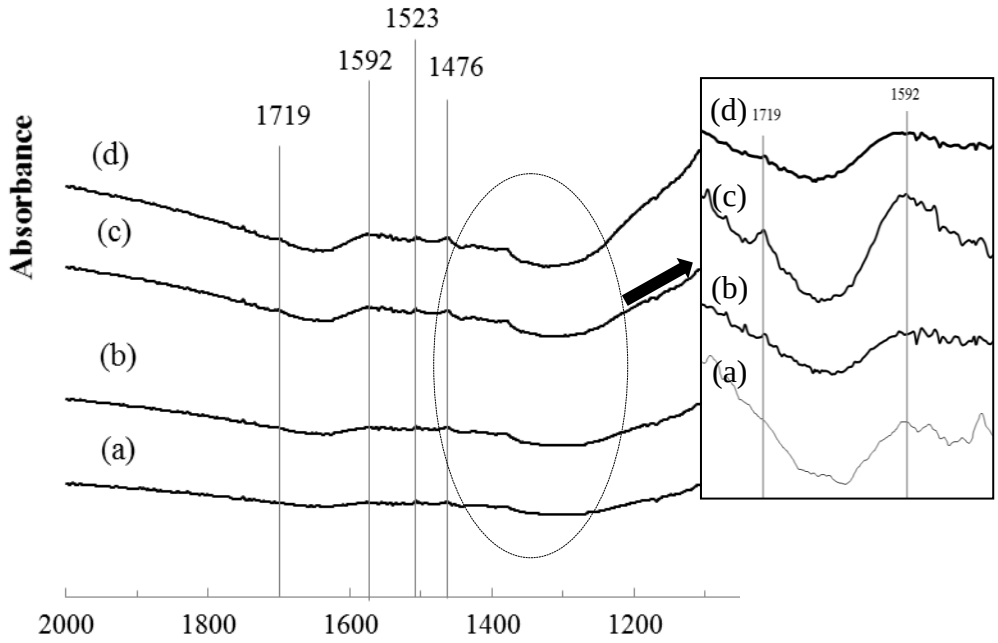

Figure 11 FTIR spectra of the prepared chars;
(a) RSC, (b) SRS500, (c) SRS800 and (d) ResC

Steam activation also significantly influenced the surface properties of the char, as presented in Table 6. Comparing with RSC, SRS500 and SRS800 had the significantly higher in BET surface and total pore volume but lower in average pore diameter. Comparing with RSC catalyst, BET surface area of SRS500 and SRS800 was increased approximately 2.46-times and 5.47-times, respectively. Steam activation at

800ºC gave the char with high porosity because the carbon oxidation was strongly promoted at high range of temperature (800 – 900ºC) resulting in the high porous char [7, 8].

Table 6 Surface properties of the fresh carbon-based catalysts by BET analyzer

	RSC	SRS500	SRS800	ResC
BET surface area (m^2 g^{-1})	62.33	153.28	341.11	34.03
BJH Mesopore surface area (m^2 g^{-1})	23.73	26.53	40.07	19.93
Micropore surface area* (m^2 g^{-1})	38.60	126.75	301.04	14.10
Total pore volume (cm^3 g^{-1})	0.0589	0.0960	0.2150	0.0545
BJH Mesopore volume (cm^3 g^{-1})	0.0459	0.0265	0.0472	0.0460
Micropore volume** (cm^3 g^{-1})	0.0130	0.0695	0.1678	0.0085
Average pore diameter (nm)	3.781	2.505	2.521	6.412

* micropore surface area was estimated by the difference of BET surface area and BJH mesopore surface area

** micropore volume was estimated by the difference of total pore volume and BJH mesopore volume

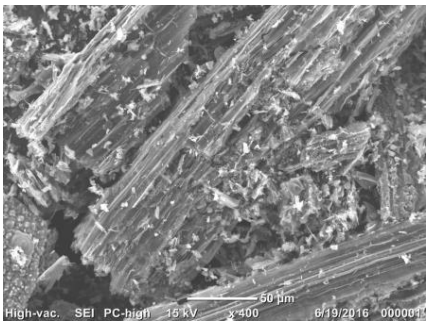

(a) RSC

(BET surface area = 62.33 m^2 g^{-1}

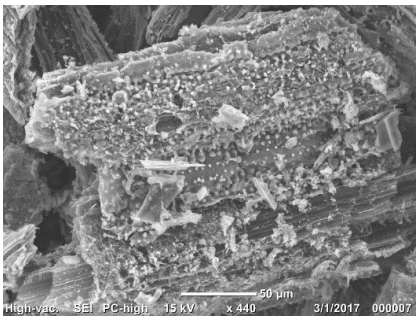

(b) SRS500

(BET surface area = 153.28 m^2 g^{-1})

(C) SRS800

(BET surface area = 341.11 m^2g^{-1})

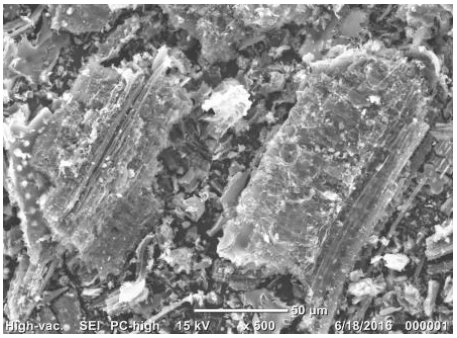

(d) ResC

(BET surface area = 42.54 m^2 g^{-1})

Figure 12 SEM images of fresh carbon-based catalysts

This result agreed with SEM images as shown in Figure 12. In case of RSC (Figure 12(a)), the surface was clearly seen as the long-channels of carbon structure with the large pores that causing by the slow pyrolysis at high temperature [9]. While, the carbon surfaces with higher porosity and smaller pore diameter were observed in cases of SRS chars (Figure 12 (b) and (c)), in particular SRS800 and. This result shows the effect of steam activation on the char surface and morphology. Moreover, inner pore structure of the chars was investigated by estimation the mesoporous surface area and mesopore volume by BJH (Brunauer-Joyner-Halenda) method by using the data from N_2 adsorption at 77 K [10]. Micropore structure of all chars were also roughly estimated by the difference between total surface area and mesopore surface area. The result is shown in Table 6. It was found that RSC contained the mixture of mesopore (pore diameter 2 -20 nm) and micropore structure (pore diameter < 2 nm), in contrast the structure of steam activated chars mostly exist with micropore structure. About 72% and 78% of total pore volume of SRS500 and SRS800 were the micropore volume. Micropore structure has been previously reported as the inductive site for coking that is the important mechanistic reaction for tar decomposition over char bed [11-13].

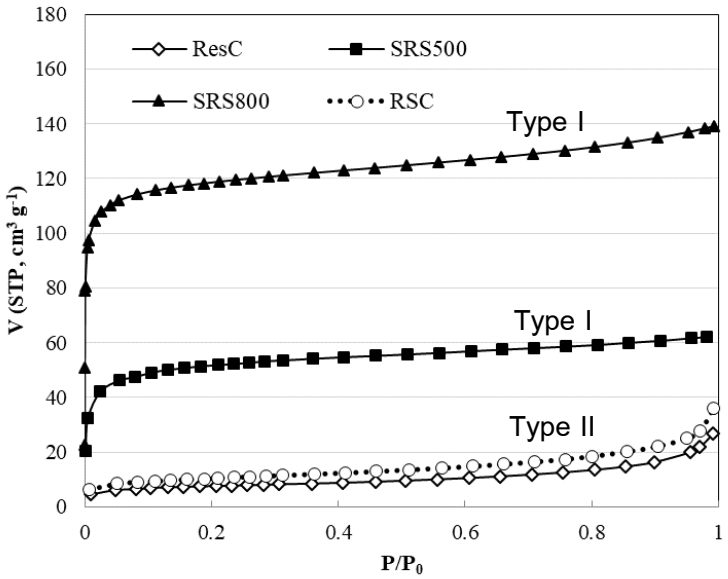

Figure 13 Adsorption Isotherm of the fresh carbon-based catalysts by N_2 adsorption at 77 K using BET analyzer

Figure 13 shows the N_2-adsorption isotherm of the fresh catalyst. From IUPAC classification of adsorption isotherm, the SRS500 and SRS800 exhibits the Type I-curve

identifying the monolayer of microporous solid with narrow range of pore diameter [14]. However, the volume of gas uptake was quite different between SRS500 and SRS800 due to the difference of surface area. Meanwhile, the RSC and ResC shows the adsorption curve Type-II refers the mixture of micropores and mesopores with different range of relative pressure (P/P_0) [14, 15].Difference properties between SRS and RSC chars would certainly influence on the catalytic activity for naphthalene decomposition, as was discussed further in the next section.

3.2.1.2 Effect of solvent treatment on the char properties

From the physical properties of the prepared chars in Table 5, it was observed that the solvent treated char (ResC) had approximately 2-times lower in mass yield comparing with RSC. While, the ash content was significantly higher (~67.9%). It can be described by the high efficiency of the degradative solvent extraction of rice straw that can produce the relatively high yield of extractable fraction (soluble and deposit) which consisting of high carbon and low oxygen contents. While, the unextractable fraction, called residue, yielded only 17wt% of raw rice straw [3]. The rice straw residue was further pyrolyzed at 800ºC in the same preparation condition with RSC that resulted to the slightly lower in mass yield (15.7 wt%). From the elemental and AAEMs analysis (in Table 2), the ResC had the lower C, Mg and Ca contents but higher in K and Si contents when comparing with the RSC. It implies that the degradative solvent extraction not only leached the carbon but also removed some alkali earth metallic species and leaving the high existence of K that mostly presented in ash as the silicate form i.e. K-Si. Silicate form of ResC was evidenced by the EDS-elemental mapping as shown in Fig. 14. For RSC (Fig. 14(a)), it could be seen that the three main elements (C, Si and K) were dispersed totally on the selected overlay surface. Some areas were the overlapping of K-Si but some areas were the dispersion of C element. On the other hand, for ResC, the overlapping of K-Si clearly appeared totally on the selected overlay surface. It was supposed that the main element composition on the ResC surface was the K-Si form, while the existence of K on the RSC was the high-active of K-bonded carbon. The formation of K on the char was the important issue influencing on the catalytic performance of the char that was discussed later.

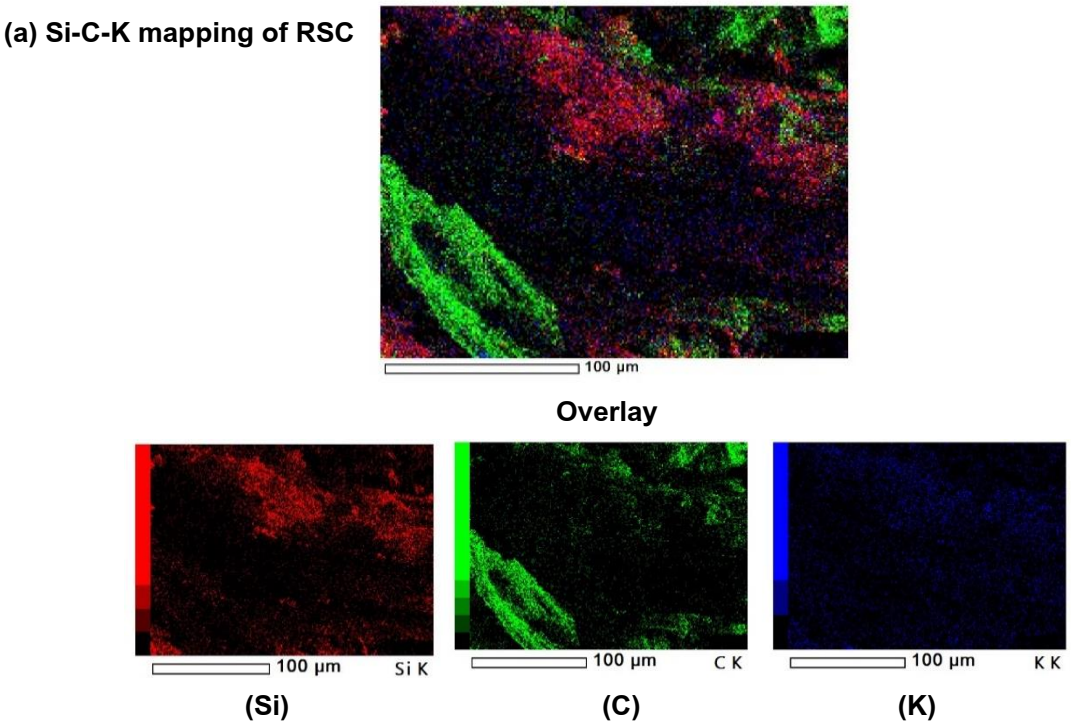

Figure 14 EDS elemental mapping by SEM-EDS of (a) RSC and (b) ResC

Consider the surface properties in Table 6, the ResC had almost 2-time lower BET surface area compared to that of RSC. It was due to the effect of high efficiency

solvent treatment to leach the enrich hydrocarbons and remain mostly the ash. Consider the inner pore structure, the ResC had the mixture of mesopore and micropore structure similarly to the RSC but the ResC had the larger average pore diameter. This result agrees with the SEM image as shown in Fig. 12(d). It clearly seen that the surface of ResC had the more condensed carbon surfaces compared to the surface of RSC and it was found the presenting of large pores.

3.2.2 Catalytic Naphthalene Decomposition

Naphthalene conversion and net gas production with and without catalysts (presence of inert alumina bed) is illustrated in Fig. 15. Note that the presented gas yield represents the net gas production after subtracting the gas generated from the catalyst itself.

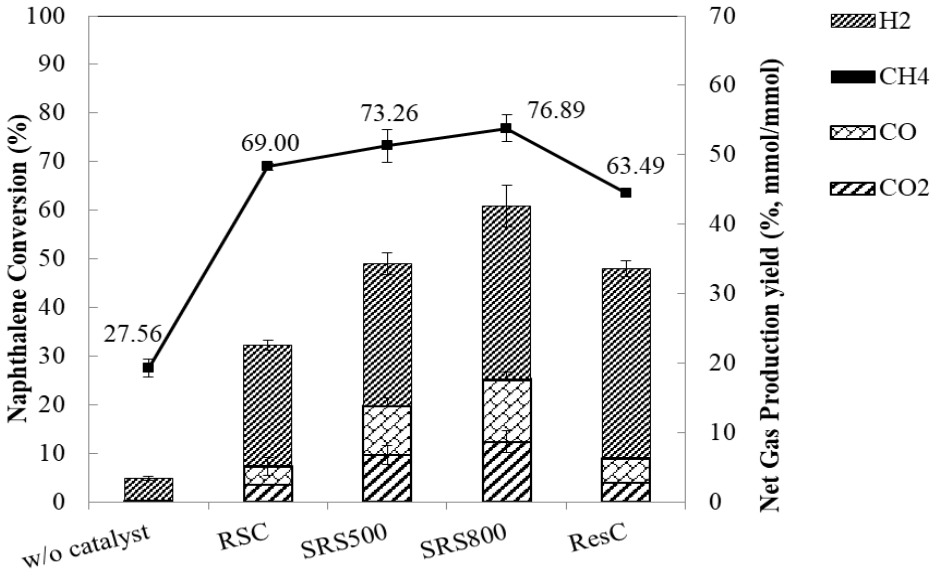

Figure 15 Naphthalene conversion and net gas yield with the presence of inert and the various types of carbon-based catalysts

Without catalyst, naphthalene conversion was only about 27% and net gas production around 5 %. Most of gas products were H_2 and traces of CH_4, C_2H_4 and C_2H_6. From the previous study [13], the overall thermal cracking of naphthalene under inert atmosphere can be expressed as Eq. (2)

$$C_{10}H_8 \rightarrow C_nH_x + C_mH_y + C + H_2 \quad (2)$$

when C_nH_x represents the smaller hydrocarbons than naphthalene, C_mH_y represents the larger molecules of tar species than naphthalene and C represents the solid coke or soot. H_2 production from the thermal cracking was the net output from the competitive reactions between dehydrogenation of the large molecules or coking and the

hydrogenation of the large molecules to smaller molecules and incondensable gas products such as CH_4 and C2-hydrocarbons. With the presence of carbon-based catalysts, naphthalene conversion and net gas production were significantly higher for all cases. It implies that the carbon-based catalyst could promote the decomposition of naphthalene under this condition (at 800ºC and inert atmosphere). Naphthalene conversion is in the following order: SRS800 (76.9%) > SRS500 (73.3%) > RSC (69.0%) > ResC (63.5%). This corresponded well with the BET surface area of the fresh catalyst (see Table 2). It could be stated that surface area of the catalyst was the dominant factor to determine the degree of naphthalene decomposition. Pore size and pore structure of the catalyst was also important. As mention in Section 3.2.1, SRS800 had the Type I-adsorption isotherm referring the high portion of micropore structure with narrow range of pore size. Micropore structure has been previously reported as the inductive sites for tar cracking as well as coking [11-13]. This might be the main reason of the highest catalytic performance of SRS800 for naphthalene decomposition. Considering in the net gas production, with the presence of catalysts, H_2 production drastically increased due to the promotion of thermal cracking of naphthalene over the catalyst surfaces. Decomposition of tar over char bed has been previously proposed for 2 steps; firstly, the deposition of tar into the porous of char to generate coke or soot and the decomposition of formed coke by thermal and/or oxidizing agents (steam/CO_2/O_2) [16, 17]. During tar deposition or coke formation, H_2 was the major product that can be significantly detected in case of SRS catalyst because of the high BET surface area and micropore structure. However, the highest H_2 production was found in case of ResC, even though the surface area was not as high as SRS catalyst. It might be due to the role of AAEM species (in particularly K) on its surface that could facilitate the decomposition of hydrocarbons to generate more H_2 and small hydrocarbon molecules such as CH_4 [12, 18]. Moreover, a large production of CO and CO_2 were observed in cases of SRS catalyst while less was observed in cases of RSC and ResC. Even though the CO and CO_2 was unexpected, they can probably be formed by interactions between oxygenated functional groups (such as C=O, COOH) on the char surface and the hydrocarbons molecules derived from naphthalene cracking. The relatively high CO and CO_2 contents in cases of SRS catalysts, especially SRS800, were corresponding with the high O/C ratio of the fresh catalyst and the presence of C=O peak from FTIR patterns.

Gas production profile as function of naphthalene feeding time with and without catalyst is illustrated in Fig. 16. The gas production profile was a good indicator to determine the extent of naphthalene decomposition over time and also determine the mechanism of each catalyst for naphthalene decomposition. Without catalyst, H_2 and CH_4 were produced almost constantly during the feeding time of 100 min with the average yield of H_2 and CH_4 of 0.3 and 0.008 mmol g^{-1}, respectively. With the presence of catalysts, gas production significantly increased for all gas species when comparing with the case in the absence of catalyst.

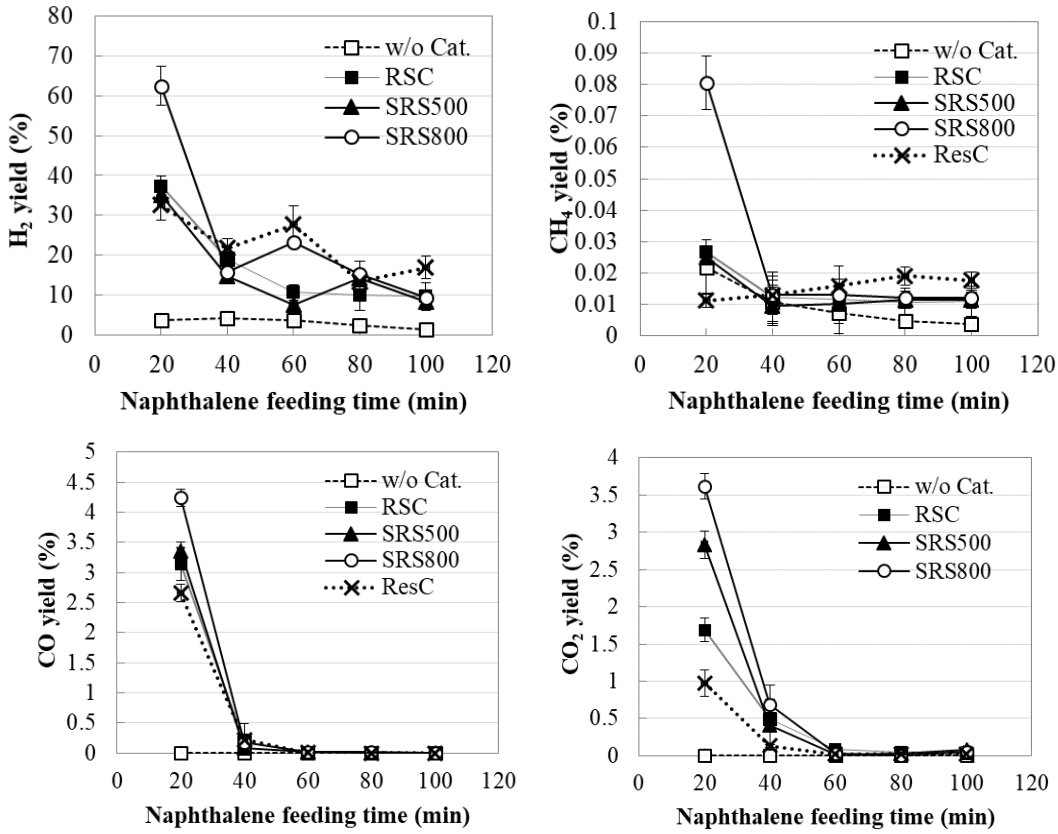

Figure 16 Gas production yield by time during naphthalene decomposition: (a) H_2, (b) CO, (c) CH_4 and (d) CO_2

Higher CO (Fig. 16(b)) and CO_2 (Fig. 16(d)) was observed at the first 20 min, in particular in the presence of SRS800. The amount of CO and CO_2 were lower within 40 min and completely disappeared after 60 min for all cases of catalysts. This indicates that all catalysts were deactivated after 60 min of feeding time. As mentioned above, CO and CO_2 were probably generated from the interaction between hydrocarbons from the cracking products and oxy-functional groups of the catalyst. After 60 min, the deactivation of catalyst probably cause by the tar deposition on the porous surfaces and

the complete loss of oxy-functional group of the catalysts. It could be clearly observed in the case of SRS800 because it had the high surface area and also had the high oxy-functional groups. An important evidence to disclose the catalyst deactivation by coking and by the loss of oxy-functional groups was the increased carbon content and decreased oxygen content of the used catalyst compared to the fresh one.

Considering in H_2 production (Fig.16(a)), it was clearly observed that in case of SRS800, H_2 was strongly generated at the first 20 min, then rapidly decreased within 40 min and kept constant until the feeding stop. This indicates that at the first 20 min, H_2 rapidly evolved by the tar deposition on the micropore of SRS800. After that the micropores were covered by coke/soot and H_2 might generate from the thermal cracking of naphthalene in the vapor phase as expressed in Eq. (2). This corresponded with the almost constant CH_4 production after 40 min of feeding time (Fig.16(c)) in case of SRS800. For SRS500, H_2 production gave a similar trend with the SRS800 but the yield of H_2 was slightly lower due to the lower BET surface area comparing with SRS800. In case of RSC, H_2 was significantly produced at the first 20 min but significantly lower than the case of SRS800 due to the less influence of tar deposition on the lower BET surface area and mesoporous structure of the RSC. However, after 20 min, the H_2 as well as CH_4 yields gradually reduced and kept constant until the feeding stopped. It was probably the effect of the thermal cracking of naphthalene in the vapor phase (Eq. (2).

With the presence of ResC, H_2 was rapidly generated at the first 20 min but lower than the SRS catalyst. This result was similar with the case of RSC due to the very close surface area and the mesoporous structure of both catalysts. However, after 20 min, it was remarkable that H_2 and CH_4 yields in case of ResC were higher than the RSC and also the SRS catalysts during the feeding time of 40 -100 min. One explanation is that the different form of AAEMs on the catalyst surface, especially K, between RSC and ResC. As mentioned in Section 3.2.1, ResC had the lower K/Si molar ratio than that of RSC. It was presumable that the existence of K in ResC might be the potassium silicates (K-Si-O), while in case of RSC, K might exist as the potassium phenolates (K-O-C). Some studies [19-21] reported that the K-phenolates was more reactive than the K-silicates for the decomposition of char and tar. Therefore, the K-phenolate group in case of RSC probably played the catalytic roles simultaneously with the thermal cracking of naphthalene to generate the high amount of H_2 during the first 60 min (see Fig.5(a)). After that the activity of K-phenolate may

probably be inhibited by the reaction with volatiles or/and hydrogen radicals from the naphthalene cracking as following Eq. (3),

$$CM - M + H \leftrightarrow CM - H + M \quad (3)$$

,where CM, H and M represent the char matrix, hydrogen radical from the volatile and AAEM species, respectively [6, 19, 22]. This might result in the lower H_2 amount after 60 min of feeding time. On the other hand, in case of ResC, the more stable form of K-silicates would probably be less influenced by volatiles. That is why in case of ResC the H_2 and CH_4 productions were higher during 40-100 min of feeding time.

3.2.3 Characterization of the spent carbon-based catalysts and the proposed mechanism

Physical properties of the used catalysts (after 100 min of naphthalene feeding) were characterized and the result is shown in Table 7.

Table 7 Physical properties of the used carbon-based catalysts

	RSC	**SRS500**	**SRS800**	**ResC**
Element analysis (wt%, daf.)				
Carbon (C)	76.7	76.3	72.1	77.4
Hydrogen (H)	1.9	1.8	2.1	1.7
Nitrogen (N)	0.7	0.6	0.2	0.0
Oxygen (O)	20.6	21.1	25.5	20.92
O/C molar ratio	0.20	0.21	0.26	0.20
Surface properties				
BET surface area (m^2/g)	31.09	16.05	65.04	7.84
Total pore volume (cm^3/g)	0.0294	0.0155	0.0610	0.0501
average pore diameter (nm)	3.786	3.880	3.756	25.58
AAEM analysis (wt% dry)*				
Potassium (K)	1.49 ± 0.08	2.24 ± 0.42	2.10 ± 0.51	1.74 ± 0.08
Magnesium (Mg)	0.45 ± 0.13	0.25 ± 0.03	0.56 ± 0.07	0.41 ± 0.13
Calcium (Ca)	1.68 ± 0.42	0.21 ± 0.05	0.48 ± 0.01	0.33 ± 0.01
Silicon (Si)	4.89 ± 0.47	11.55 ± 0.53	16.25 ± 0.81	11.60 ± 0.93
K/Si molar ratio	0.22	0.14	0.09	0.11

* by SEM-EDS determine by the average data from at least 3 areas analysis with SD

It was observed that all used catalysts had the higher carbon content but lower oxygen content when comparing with the fresh catalysts. Carbon content significantly increased from 54.6 to 72.1 wt%, while the oxygen content significantly decreased from 41.9 to 25.5 wt% in the cases of SRS800. It was strongly suggested that the carbon deposition (coking) from volatiles was extremely promoted over the SRS800 catalysts resulting in the increase of H_2 production, especially at the early stage of naphthalene decomposition, as previously explained in Section 3.2.2. Coke deposition was also confirmed by the reduced BET surface area and pore volume of the used catalyst. BET surface area of the SRS500, SRS800 and ResC catalysts was significantly decreased from 153.28, 341.11 and 42.54 m^2g^{-1} to 16.05, 65.04 and 7.84 m^2g^{-1}, respectively. Change of morphology of the fresh and used catalyst was the one evidence to clarify the deactivation of the catalyst and the result is shown in Fig. 17. Comparing with the fresh catalyst, morphology of all catalyst was drastically changed from the high porous surfaces into the dense-carbon surfaces, in particular the SRS800 (Fig.17 (e) and (f)) and ResC (Fig.17 (g) and (h). This result corresponds with the reduction of BET surface area of the used catalyst as mentioned previously. Nestler et al. [23] and Hosokai et al. [24] investigated the structure change of wood char during the naphthalene or biomass tar decomposition. They reported that structure change of the used carbon-based catalyst was caused by the coverage of hydrocarbon on the porous surface. Considering in the AAEM content of the used catalysts in Table 3, it was observed that K content for all used catalysts were strongly reduced when comparing with the fresh ones (in Table 2), especially in cases of RSC and ResC. The K/Si molar ratio was also reduced due to the increase of Si fraction in the used catalysts. This result confirms that the catalytic roles of RSC and ResC were strongly influenced by the transformation of AAEM during the reaction.

Mechanism of the SRS catalyst for naphthalene decomposition could be explained by the high surface area and the existence of micropore surface that could promote tar deposition to generate coke and H_2 at the early stage. In parallel, the high portion of oxy-functional groups of the SRS catalyst was the main factor that could interact with the volatiles from naphthalene cracking and then possibly produce high amount of CO and CO_2. However, after 60 min left, the SRS was completely deactivated by coking and the active oxy-functional groups were almost lost.

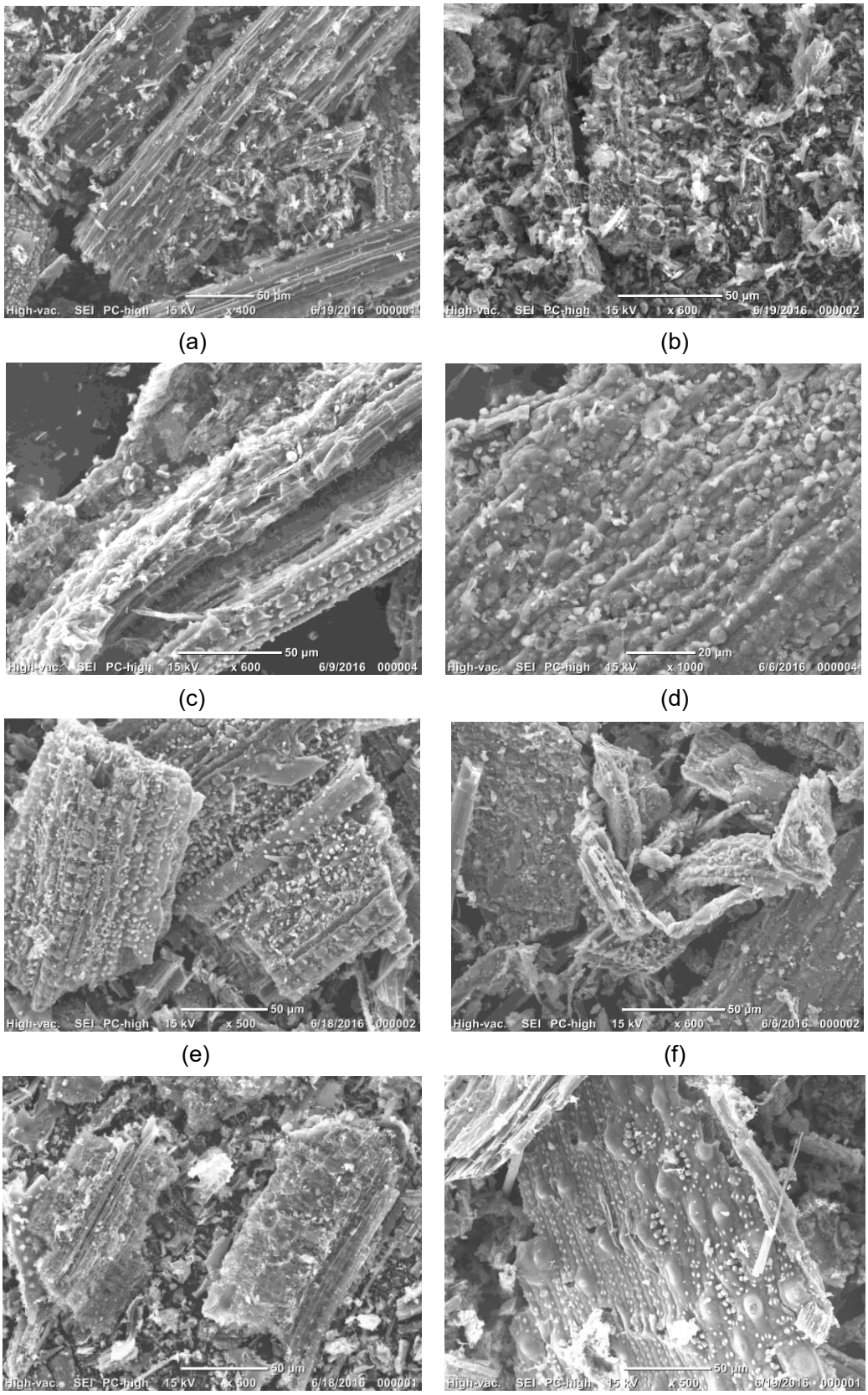

Figure 17 Change of morphology of the carbon-based catalyst by SEM: (a) fresh RSC (500X)**,** (b) used RSC (600X), (c) fresh SRS500 (500X), (d) used SRS500 (1000X), (e) fresh SRS800 (500X), (f) used SRS800, (g) fresh ResC (500X) and (h) used ResC (500X)

However, the detected small production of H_2 and CH_4, thermal cracking of naphathalene in vapor phase continued until the feeding stop. Mechanism of RSC and ResC for naphthalene decomposition was quite different from SRS catalysts. Due to the low BET surface area/pore volume and the presence of mesoporous structure of the RSC and ResC catalysts, the tar deposition to form coke and H_2 was less dominant when comparing with the SRS catalysts. On the other hand, the high proportion of AAEMs both in cases of RSC and ResC was the major key to catalyze naphthalene cracking. From these results, it can be stated that the different type of catalyst would play the different catalytic roles for naphthalene deposition depending on their major characteristics. This would be useful for the design and preparation of the active carbon-based catalysts for the decomposition of tar.

3.3 Conclusion

Decomposition of naphthalene over the rice straw derived carbon-based catalysts were examined in a lab-scale fixed bed reactor. Effects of steam activation and solvent treatment during catalyst preparation were investigated and the catalytic mechanism of each catalyst were determined from the characterization of fresh and used catalysts. Results shows that, with the presence of all carbon-based catalysts, the higher naphthalene conversion and higher net gas production were observed. Steam activated char at 800ºC (SRS800) was the best catalyst to give the highest naphthalene conversion of 76.9% and the highest net gas production about 45%. The major catalytic key of the SRS was the enhancement of BET surface area and pore volume as well as the micropore structure by steam activation that inducing the tar deposition to generate coke and H_2 during the early stage of naphthalene cracking. In the same time, the higher amount of active oxy-functional groups of SRS by steam activation was also an important key to produce the high yields of CO and CO_2 during the naphthalene decomposition. However, the SRS was more rapidly deactivated by coking and the loss of oxy-functional groups than that the other catalysts. On the other hand, rice straw char (RSC) and solvent treated rice straw char (ResC) had the lower catalytic activity than that of SRS catalysts due to the lower BET surface area and pore volume as well as the mesoporous structure. However, ResC gave the highest H_2 production, in particular after 40 min of feeding time because of the catalytic activity of K species on tar decomposition in the silicate form (K-Si). The outcome from this study could be further applied for the design and preparation of the active carbon-based catalysts for biomass derived tar decomposition.

3.4 Output and publications

International Journal

Supachita Krerkkaiwan and Suneerat Fukuda. “Catalytic effect of Rice Straw derived Chars on the Decomposition of Naphthalene: Influence of steam activation and solvent treatment during char preparation” (in preparation)

International Conference

Supachita Krerkkaiwan and Suneerat Fukuda. “Decomposition of Naphthalene over Rice straw derived carbon-based catalysts: Influence of steam and solvent during catalyst preparation” Poster presentation in **TRF-OHEC Annual Congress 2017 (TOAC2017)** which held in The Regent Beach Cha-am, Petchaburi, during 11- 13 January 2017**.**

4. Details of Part 3: Catalytic performance of the carbon-based catalyst on the decomposition of biomass derived tar

4.1 Material and Method

4.1.1 Biomass Sample and Char Preparation

Rice straw (RS) and *Leucaena leucocepha* wood (LN) are the biomass used in this study. They were ground, sieved to a 150–250 μm size, dried at 110^{o}C for at least 6 h and kept in a desiccator before use. Char was prepared from the slow heating pyrolysis of coal, biomass and coal/biomass blend in a typical fixed-bed reactor as previously reported in reference [20]. Pure biomass chars (RSC or LNC) were prepared from RS or LN with the particle size of 150–250 μm. Co-pyrolyzed chars (C/RS or C/LN) were prepared from the co-pyrolysis of the Indonesian sub-bituminous coal and biomass at coal and biomass blending ratios of 1:1 (w/w). For all chars, 7 g of original sample was placed inside the quartz reactor (20 mm-ID and 40 cm heating zone length) and then slowly pyrolyzed under nitrogen (N_2) flow rate of 120 mL/min. Heating program during char preparation was set as following: heating from room temperature to 600ºC with 10 ºC/min of heating rate and held at 600ºC for 60 min.

4.1.2 Decomposition of Biomass derived Tar in a Two-Stage Fixed Bed Reactor

Decomposition of biomass derived tar was performed in a two-stage fixed bed reactor (Fig. 18) that consists of an inner tube (9 mm-ID and 60 cm-length) and an outer tube (19 mm-ID and 89 cm-length). The reactor was divided into two parts; upper and lower parts, which the temperature was individual controlled by each electrical furnace (Upper furnace: Carbolite model MTP 12 and lower furnace: Lenton model LTF 12). The upper part was “pyrolysis zone” where the biomass pyrolysis took place and

generated the volatiles. The lower part was “tar steam reforming zone” where the prepared char or/and inactive alumina ball (inert bed) was located, steam was fed and the biomass derived volatiles from the upper part was reformed into gas.

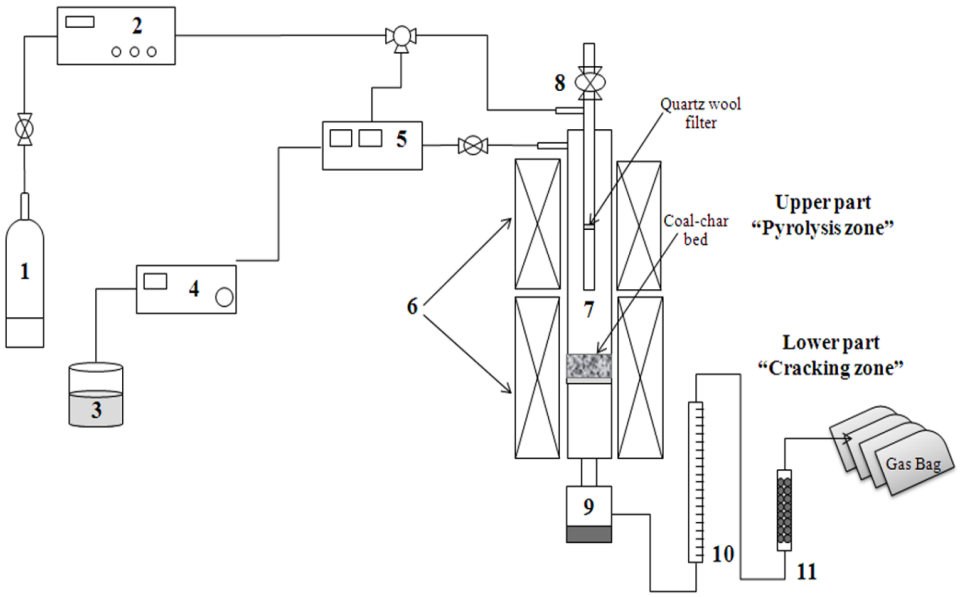

Figure 18 Schematic diagram of a two-stage fixed bed reactor which consists of (1) Nitrogen cylinder, (2) Mass flow controller, (3) Distillated water reservoir, (4) HPLC pump, (5) Steam temperature controller, (6) Electric Furnaces, (7) Quartz reactor, (8) Sample feeder, (9) Iced-tar trap, (10) Bubble flow meter and (11) Moisture trap (filled with silica gel)

Steam reforming started from the packing of about 0.5 g of the prepared char or 7.5 g of inert bed into the lower part of the reactor with the bed height of 2 cm. Then N_2 was fed into the reactor with flow rates of 80 and 30 mL min^{-1} for the inner and outer tubes, respectively. Residence time of volatile through the char bed was approximately 0.3 sec. After purging for 1 h, the upper electric furnaces at pyrolysis zone were heated up to the desired temperature (600, 700 or 800^{o}C), in the same time, the temperature at tar steam reforming zone was heated up to 800ºC for all experiments. Water (liquid) with flow rate of 0.14 µL min^{-1} was heated at 300ºC. The steam was introduced into the lower part of the reactor at a steam/N_2 (v/v) ratio of 60/40. Simultaneously, 120 mg of fresh biomass was dropped into the inner tube at the upper part. The obtained biomass char remained on the quartz wool filter in the middle of the inner tube, while only the biomass volatiles passed into the lower part. At the lower part, the biomass volatiles make contacting with steam and the char allowing the catalytic tar reforming to take

place. The mass ratio of biomass feeding and char bed was kept constant at 1:4.2 (g:g) for all experiments.

Some of the heavy tars were condensed in an iced-tar trap filled with isopropanol and 6 mm diameter-round glass beads to enhance its capability for recovering the condensable compounds. Non-condensed (gaseous) products were then collected in a 2 L-gas bag for quantitative analysis. The gas collection bag was changed every 10 min during the 1 h reaction time. The gaseous products generated from the char in the lower part without biomass feeding was evaluated in the same manner and used as the reference data ("blank experiment").

Carbon conversion into gas was determined following Eq. (4),

$$\textit{Carbon conversion (\%)= C in product gas / C in biomass feed} \quad (4)$$

where *C in product gas* represents the mole of carbon in gas product and *C in biomass feed* represents the mole of carbon in biomass. Carbon conversion into char was obtained from the carbon content of biomass char remained in the inner tube at upper stage by CHN analyzer. Consequently, the carbon conversion into tar was calculated following Eq. (5),

$$\textit{Carbon conversion into tar (\%)} = 100 - C_{gas} - C_{char} \quad (5)$$

where C_{gas} and C_{char} represent the carbon conversion into gas and char, respectively.

4.1.3 Characterization of Sample and Products

Proximate and ultimate analyses of raw coal, raw biomass and char samples (CC, C/RS, C/LN, RSC and LNC,) were performed following ASTM D3172-3175 and using a CHN analyzer (LECO CHN-2000), respectively. Moreover, the specific surface area, average pore volume and average pore size of the chars were measured by N_2 adsorption at -196 ^{O}C using the BET method (model Quantachrome, Autosorb-1, instrument accuracy ± 0.11%). Samples were first degassed at 300ºC for 12 h prior to the N_2 adsorption. Morphology of the chars was characterized by SEM (model JEOL, JSM-5410LV). Mineral analysis of the chars were also performed by X-ray fluorescence (XRF, BRUKER model S8Tiger) technique. Gas product, mainly comprises of H_2, CO, CH_4 and CO_2, was quantitatively analyzed by gas chromatography (GC) using a Shimadzu GC-2014 model with a thermal conductivity detector (TCD) and Unibeads C column (3.00 mm ID × 200 cm length).

Some of the condensable tar in the ice-tar trap was analyzed to determine its chemical composition using GC-mass spectrometry (MS) on a Shimadzu Model QP2010 equipped with a DB-5ms capillary column (0.25 mm-OD × 0.25 mm film thickness, 30 m

length, J & W Scientific) and with helium as the carrier gas. The molecular weight scan range was 30–500 m/z with a 3.5 min solvent cut time. The column was held at 40 °C for 5 min, and then the temperature was increased to 200 °C at rate of 10 °C/min and held for 25 min.

4.2 Result and discussion

4.2.1 Characterization of Coal, Biomass, Prepared Chars and Tar product

Table 8 summarizes the proximate and ultimate analyses of raw coal and biomass samples. It was found that comparing with coal, biomass samples both rice straw (RS) and Leucaena leucocepha wood (LN) had about 2-times higher in volatile matter (~62%), while fixed carbon was lower. From ultimate analysis, SB coal had about 72 wt% of carbon content that higher than that of both biomass samples, while oxygen content of SB coal was lower resulting in the lower O/C molar ratio. Coal also had a relatively high sulfur content due to the low-rank coal characteristics.

Table 8 Proximate and ultimate analyses of raw coal and biomass samples

	Sub-bituminous coal	**Rice straw (RS)**	**Leucaena leucocepha (LN)**
Proximate analysis (wt%, dry basis)			
Moisture	12.4	6.4	8.9
Ash	8.4	11.2	2.6
Volatile matter	36.8	61.9	62.2
Fixed carbon	42.4	29.2	26.3
Ultimate analysis (wt%, daf.)			
Carbon (C)	72.1	45.3	48.4
Hydrogen (H)	6.7	6.9	7.1
Nitrogen (N	1.4	0.9	0.3
Sulfur (S)[a]	0.22	0.14	0.14
Oxygen (O)[b]	19.6	46.7	44.1
H/C molar ratio	1.1	1.8	1.7
O/C molar ratio	0.2	0.8	0.7

The difference of chemical properties of coal and biomass samples were significantly influenced on the properties of the prepared chars that presented in Table 9. Five types of char were prepared at the same pyrolysis condition (600ºC, 60 min holding time) following the preparation method as described in Section 4.1.1. Results revealed that coal char (CC) had a relatively higher in carbon content but lower in oxygen content than that of the biomass chars resulting in the lower in O/C molar ratio. While, the coal/biomass blended chars (C/RS and C/LN) showed the middle values of carbon, oxygen contents and O/C molar ratio between the values of CC and biomass char. Consider the effect of biomass type, LNC and CLN had the lower O/C molar ratio than that of RSC and CRS chars, respectively due to the different characters of woody biomass (LN wood) and agricultural based biomass i.e. rice straw.

Table 9 Physical properties of the prepared char samples

	CC	CRS	RSC	CLN	LNC
Ultimate analysis (wt%, daf.)					
Carbon (C)	84.6	70.2	54.6	81.7	77.0
Hydrogen (H)	2.9	2.33	1.6	2.6	1.8
Nitrogen (N	1.4	1.3	1.1	1.3	0.9
Oxygen (O)[a]	11.2	26.2	42.7	14.5	20.2
H/C molar ratio	0.41	0.40	0.36	0.38	0.28
O/C molar ratio	0.10	0.28	0.59	0.13	0.20
Mineral analysis (wt%, dry char sample)[b]					
Silicon (Si)	1.58	5.24	6.20	2.19	0.44
Potassium (K)	0.075	1.04	2.15	0.596	1.81
Calcium (Ca)	0.53	0.48	0.53	0.67	1.27
Magnesium (Mg)	0.098	0.145	0.158	0.134	0.145
Surface properties					
Average BET surface area (m^2 g^{-1})	180.3	283.8	180.2	276.3	208.6
Total pore volume (m^3 g^{-1})	0.139	0.175	0.129	0.146	0.087
Average pore size (A^o)	27.68	27.99	34.05	27.74	29.14

[a] by difference, [b] by X-ray diffraction (XRF)

Consider in mineral analysis reporting on the basis of char samples, it showed that CC contained a relatively low content of mineral, while biomass char and coal/biomass chars had the higher mineral contents. For rice straw, RSC as well as CRS had the very high in Si and K contents. It indicates that the mineral in rice straw could be allocated into the CRS char during the co-pyrolysis with coal. In contrast, for LNC and CLN, the main mineral were K and Ca. These mineral compositions of the char are the significant factor influencing on the catalytic performance on tar steam reforming that would be discussed in the next Section. Surface properties of the prepared chars were also reported as the average BET surface area, total pore volume and average pore size. It revealed that CC and RSC had the very close surface area and total pore volume but RSC had a larger average pore size. It was probably due to the different macrostructure of coal and rice straw. While, CRS had a higher BET surface area and total pore volume than those of CC and RSC. This indicates the synergy effects during the co-pyrolysis of coal and rice straw. It was previously reported as in [20] about the enhancement of BET surface area of the co-pyrolyzed char between coal and biomass. However, the synergetic improvement of surface area was not observed in C/LN. It is clearly that the improvement of surface area of coal/biomass blended char significantly depends on biomass type as well as biomass to coal ratio. In our previous study [21], the BET surface area of char from co-pyrolysis of sub-bituminous coal and LN wood was lower than the predicted values at the high biomass to coal blending ratio. It was probably because the excess of volatile from biomass might diminish the reactivity of the blend char that may relate to the change of surface area and morphology.

SEM images of the prepared chars is illustrated in Fig. 19. Comparing with CC and RSC, the morphology of CRS was significantly changed from the dense of carbon surfaces into more porous structure that consistent with the increase of BET surface area. Similarly, CLN surface structure was also changed into the more porous surface after co-pyrolyzed with coal. This result had a good agreement with our previous studies [20] that also reported the higher porosity of the coal/biomass blend chars by the synergetic effect between coal and biomass during co-pyrolysis. Difference in surface properties of the chars would influence on its catalytic performance for tar steam reforming that will be discussed in the next section.

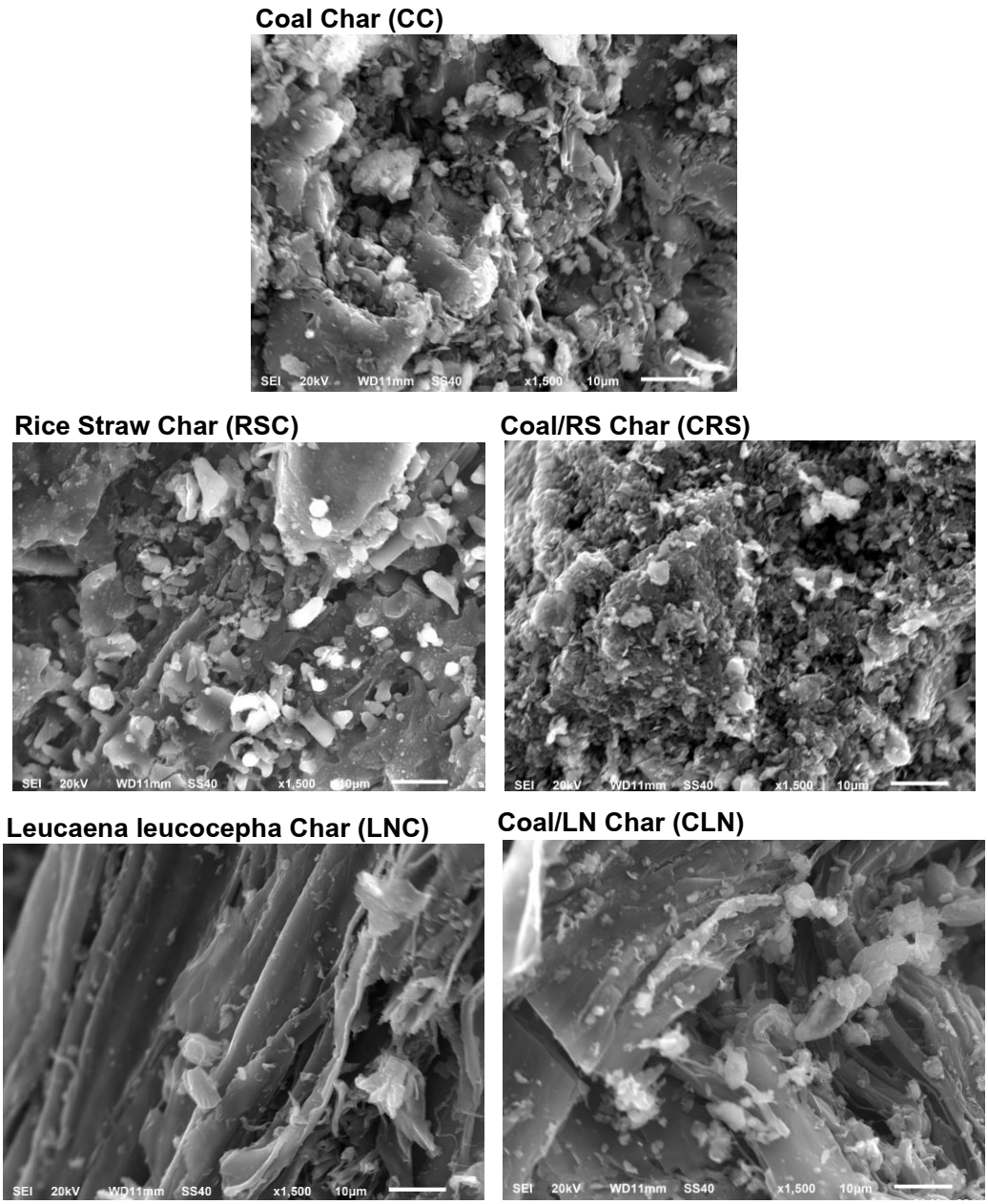

Figure 19 SEM images of the prepared char samples

Moreover, the compositions of tar at different pyrolysis temperature was characterized by GC/MS and the results are presented in Table 10 and 11 for RS tar and LN tar, respectively.

Table 10 Composition of rice straw derived tar (RT) by GC/MS with different devolatilization temperature

			Relative intensity (%)		
No.	***RT (min)***	***Compound name***	***RT600***	***RT700***	***RT800***
1	5.18	1-hydroxy-2-Butanone	1.15	-	-
2	5.21	Toluene	-	4.72	4.91
3	7.18	Furfural	6.02	2.02	-
4	7.63	3-methyl, 2-Butanone	1.03	-	-
6	7.8	5-methyl-5-Hexen-2-one	1.74	-	-
7	8.31	p-Xylene	-	2.16	1.37
8	8.37	2-(1-methylethoxy), Ethanol	2.58	-	
9	8.87	Styrene	-	4.54	6.12
10	9.12	2-methyl, 2-Cyclopentenone	2.51	0.89	-
11	9.24	1-(2-furanyl), Ethanone	1.01	-	-
12	9.57	1,2-Cyclopentanedione	1.34	-	-
13	10.45	5-methyl, 2-Furancarboxaldehyde	2.73	-	-
14	10.83	Phenol	6.93	6.08	6.24
15	11.14	1-Decene	1.25	0.57	-
16	11.22	Benzofuran	2.2	3.61	2.43
17	12.18	Indene	2.39	4.68	8.50
18	12.27	2-methyl, Phenol	3.71	12.29	1.66
19	12.4	Acetic acid, phenyl ester		4.50	4.1
20	12.67	2-methyl, Phenol	4.75	3.87	2.23
21	13.95	2,6-dimethyl, Phenol	1.58	-	-
22	14.09	3-methyl, 1H-Indene	1.46	1.80	1.25
23	14.23	4-ethyl, Phenol	3.27	-	-
24	14.37	4-Dihydronaphthalene	-	0.62	0.35
25	14.63	1,2-Benzenediol	4.64	-	-
26	14.72	Naphthalene	-	5.11	17.2
27	15.06	2,3-dihydro, Benzofuran	7.26	4.51	2.26
28	16.43	2-methyl, Naphthalene		2.69	3.97
29	16.66	1-methyl, Naphthalene		1.90	2.87
30	18.32	Biphenyl	-	0.91	1.4
31	18.61	Acenaphthylene	-	0.96	3.3
32	20.31	Fluorene	-	0.67	0.5

Table 11 Composition of Leucaena leucocepha derived tar (LT) by GC/MS with different devolatilization temperature

			Relative intensity (%)		
No.	***RT (min)***	***Compound name***	***LT600***	***LT700***	***LT800***
1	5.23	Toluene	-	6.60	5.29
2	6.2	Propanoic acid, 2-oxo-, methyl ester	1.44	-	-
3	7.37	Furfural	5.34	-	-
4	7.79	Diisopropyl 2-oxomalonate	2.26	-	-
5	7.94	Ethanol, 2-(1-methylethoxy)-	1.54	-	-
6	8.03	Ethylbenzene	-	1.14	0.46
7	8.32	p-Xylene	-	0.55	0.89
8	8.92	Styrene	1.71	7.41	7.43
9	9.19	2-methyl-2-Cyclopentenone	1.68	-	-
10	9.65	1,2-Cyclopentanedione	1.41	-	-
11	10.52	5-methyl,2-Furancarboxaldehyde	1.00	-	-
12	10.85	Phenol	4.51	11.73	5.84
13	11.25	m-methyl, Styrene	1.83	2.92	2.86
14	12.22	Indene	3.08	8.54	14.88
15	12.3	2-methyl, Phenol	4.43	5.46	1.41
16	12.68	4-methyl, Phenol	4.5	5.41	1.39
17	13.96	2,4-dimethyl, Phenol	1.85	0.84	-
18	14.62	1,2-Benzenediol	10.64	0.36	-
19	14.73	Naphthalene	1.22	7.48	21.29
20	15.06	2,3-dihydro, Benzofuran	1.61	0.95	0.32
21	15.21	1,4-Benzenediol, diacetate	3.20	1.52	
22	16.45	2-methyl, Naphthalene	0.95	2.39	2.74
23	16.66	1-methyl, Naphthalene	-	1.73	2.08
24	18.61	Acenaphthylene	-	1.67	3.26
25	20.31	Fluorene	-	0.42	0.83
26	22.98	Phenanthrene	-	1.13	0.88

It was observed that at 600ºC RS tar mainly composed of the ketone, alcohol and aldehyde functional groups, furfural and phenol derivatives as similar with the LN tar (Table 11). With increasing pyrolysis temperature (from 600 to 800ºC), oxygenated compounds (ketones, aldehyde and alcohols) significantly decreased, while the aromatic compounds such as naphthalene, methyl-naphthalene and acenaphthylene increased.

This different tar composition would be influenced on the tar steam reforming (at the second stage) that would be discussed in the next section.

4.2.2 Effect of devolatilization temperature on Non-catalytic tar steam reforming

Effect of the devolatilization temperature on the carbon conversion during the non-catalytic tar steam reforming (without catalyst) is shown in Fig.20.

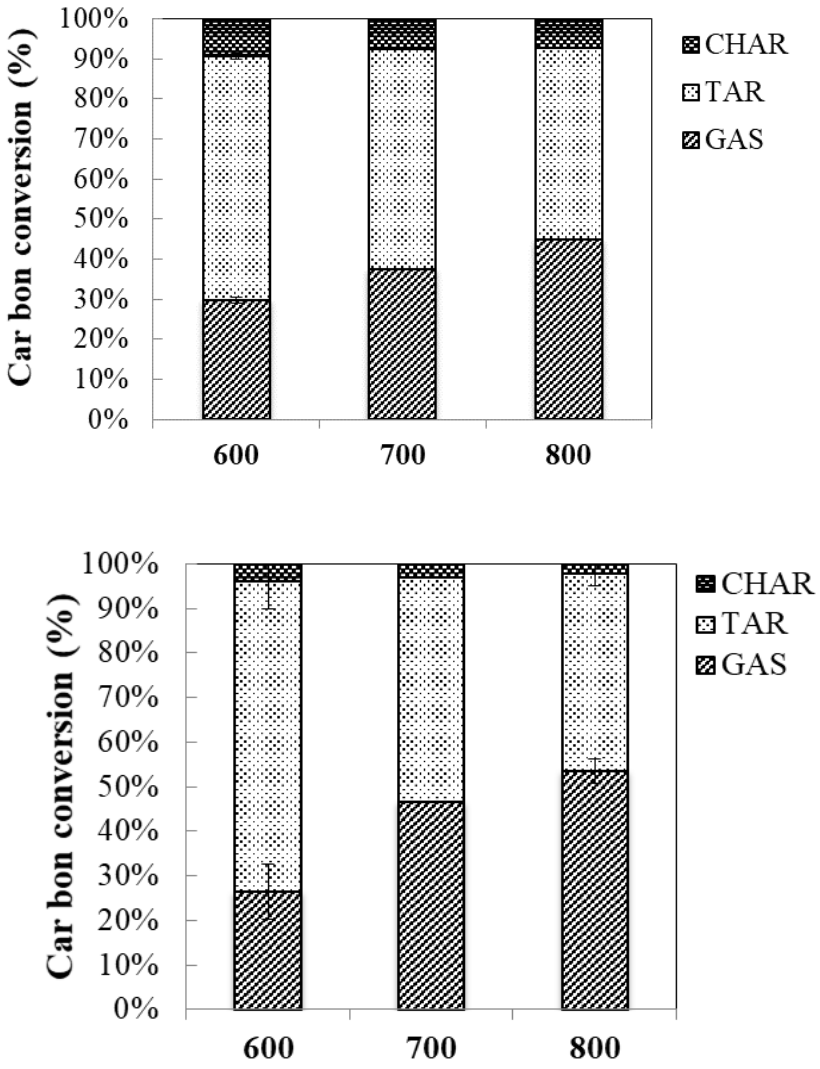

Figure 20 Effect of devolatilization temperature on carbon conversion from steam reforming of (a) rice straw derived tar and (b) Leucaena leucocepha (LN) derived tar without catalyst

Surprisingly, it was found that with the increasing of devolatilization temperature, carbon conversion into tar and char decreased but carbon conversion into gas increased significantly both RS and LN cases. From tar characterization, with higher devolatilization temperature, more stable composition such as naphthalene was the main component in tar that expected to hardly decompose into gas product. To clarify

this point, the additional experiment of biomass pyrolysis has been done and the pyrolysis products (char, tar and gas) was also collected. The result showed that carbon conversion into tar essentially decreased from 62% to 57%, while carbon conversion into gas significantly increased from 29% to 35% when the devolatilization temperature increased from 600 to 800 ºC for RS pyrolysis. Similarly, when the pyrolysis temperature increased from 600 to 800 ºC, carbon conversion into tar decreased from 70% to 46% but carbon conversion into gas increased from 26% to 52% in case of LN pyrolysis. It refers that for non-catalytic tar steam reforming, the composition of tar was not dominantly influenced on the product distribution. But, the yield of tar and gas generated from the first pyrolysis stage was the dominant effect. In the same word, it could be stated that after pyrolysis in the first stage both pyrolysis gas and tar could be reacted with steam in the second stage. Considering in the effect biomass type, it was found that no more different result was observed between RS and LN at the devolatilization temperature of 600ºC. However, at the pyrolysis temperature 700 and 800ºC, steam reforming of LN derived tar was more promoted than that case of RS derived tar as can be seen the higher carbon conversion into gas.

Figure 21 shows the effect of devolatilization temperature on gas production during the no-catalytic steam reforming of RS and LN. Four gas species consisting of H_2, CO, CH_4 and CO_2 were detected as the main composition in gas product. With the presence of steam, the complexed hydrocarbons in volatiles that generated from the first step pyrolysis could react with steam and produce high amount of H_2 and CO as following Eq. (6) or/and (7). Some oxygenated hydrocarbon molecules presenting in the gas phase could be decompose via decarbonylation and decarboxylation, as following Eq. (8) – (10) to produce high CO and CO_2 yield.

Steam reforming of carbon and Methane

$C + H_2O \longleftrightarrow CO + H_2$ Eq. (6)

$CH_4 + H_2O \longleftrightarrow CO + 3H_2$ Eq. (7)

Decarbonylation and decarboxylation

$COR \longleftrightarrow CO + R$ Eq. (8)

$RCOH \longleftrightarrow CO + RH$ Eq. (9)

$RCOOH \longleftrightarrow CO_2 + RH$ Eq. (10)

,where R= hydrocarbon radicals

With increasing the devolatilization temperature, H_2 and CO were significantly increased, while CH_4 and CO_2 showed a slightly higher both in cases of RS and LN. It was probably due to at higher devolatilization temperature the higher amount of volatiles were produced from the first stage and then react with steam at the second stage via steam reforming to generate high H_2 and CO products. Consider the effect of biomass type, LN shows the slightly higher H_2 and CH_4 yields but significantly higher in CO and CO_2 than that of RS. From the composition of tar (in Table 3 and 4), it was found that LN tar composed of a higher phenolic compounds i.e. phenol and methyl phenol than that of RS tar resulting in the boosting of tar decarbonylation reaction (Eq. (8)-(9)).

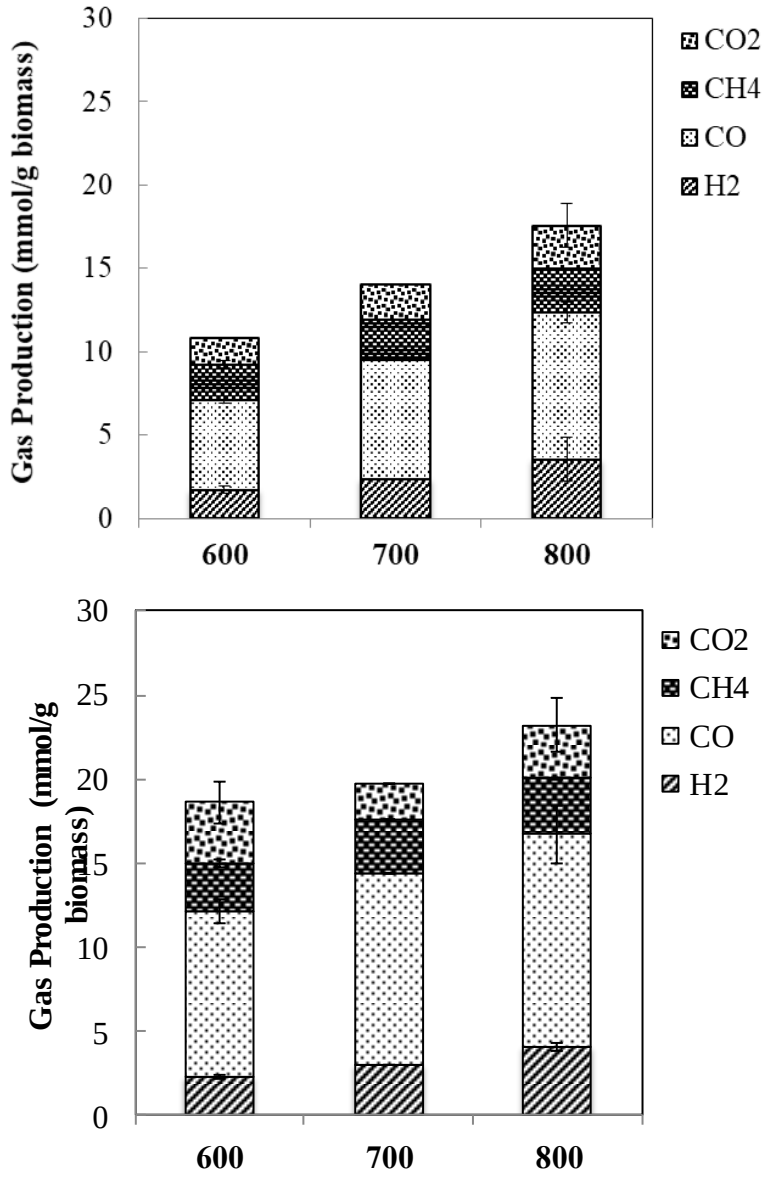

Fig. 21 Effect of devolatilization temperature on gas production from steam reforming of (a) rice straw derived tar and (b) Leucaena leucocepha (LN) derived tar without catalyst

4.2.2 Effect of devolatilization temperature on Catalytic tar steam reforming

Effect of devolatilization temperature on carbon conversion of the catalytic tar steam reforming of RS and LN is illustrated in Fig. 22. As expected, with the presence of all chars, the carbon conversion into gas dramatically increased while carbon conversion into tar decreased significantly when comparing with non-catalytic tar steam reforming (without char). Surprisingly, with the presence of all catalysts, the tar released at pyrolysis temperature of 700ºC shows the highest carbon conversion into gas followed by the tar released at pyrolysis temperature of 800 and 600ºC, respectively. This result was inconsistent with the case of non-catalytic tar steam reforming as described in Section 4.2.1. It is clearly stated that the presence of char resulted somewhat different mechanism for tar steam reforming. As formerly described, GC-MS of tar generated from the pyrolysis at 700ºC consisting of phenolic compounds and single-ring aromatic derivatives like methylbenzene, while the tar generated at 800 ºC mainly comprised of 2- or 3-rings aromatic compounds. It was probably concluded that all prepared chars in this study (C/RS, C/LN, RS and LNC) favors to promote the steam reforming of tar which containing the high content of phenolic compounds rather than the 2- or 3-ring aromatic hydrocarbons or PAHs.

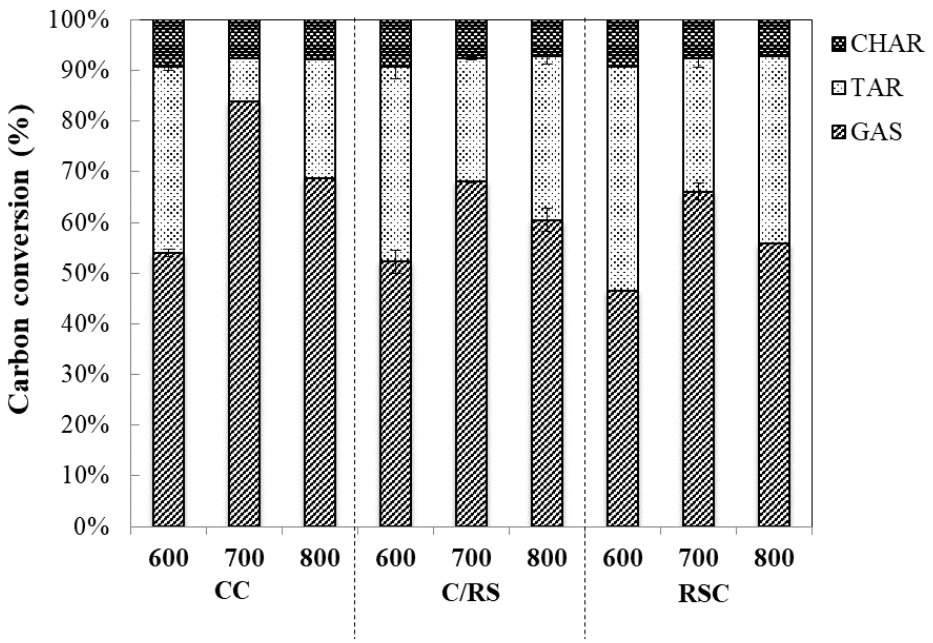

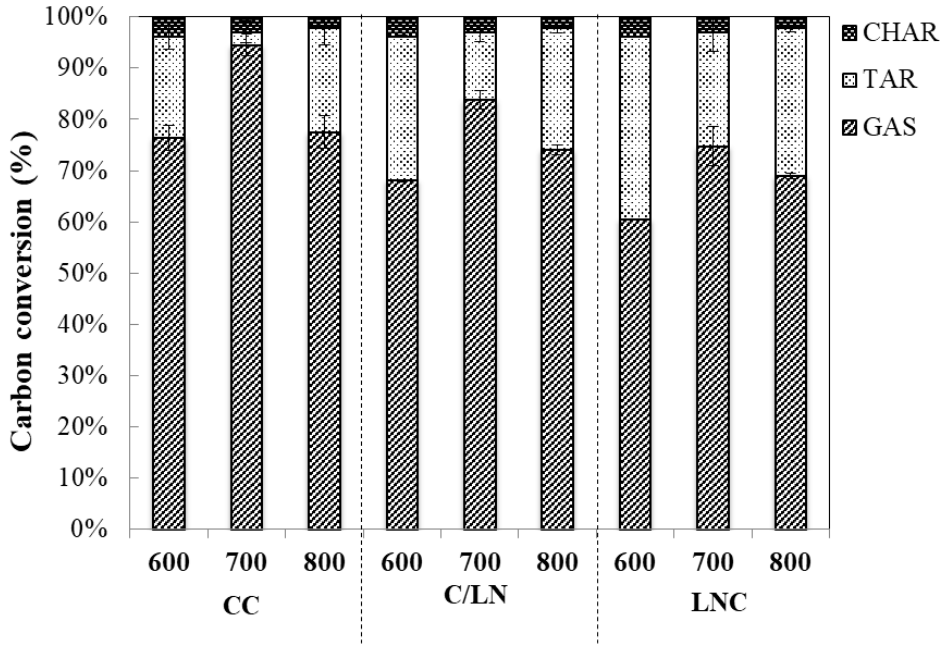

Fig. 22 Effect of devolatilization temperature on carbon conversion from steam reforming of (a) rice straw derived tar and (b) Leucaena leucocepha (LN) derived tar with catalyst

Table 12 shows the BET surface area of the catalyst after tar steam reforming. It was found that in “blank” experiment (no biomass feeding) all catalysts shows the relatively high BET surface area and total pore volume and also higher than the BET surface area of the fresh catalyst. It was clearly identify that the catalyst was extremely activated by steam at 800ºC, especially LNC showing the highest BET surface area as high as 723.6 m^2 g-1. This has agreement with Ref. [8] that reported the higher BET surface area of biomass char after activation by steam at the relatively high temperature. After tar steam reforming, all spent catalysts had the lower BET surface area due to the deposition of tar generated from the pyrolysis stage or coke formation. Many researches proposed the mechanism of char catalyzed tar decomposition under volatile-char interaction [13, 16, 24, 25] .Decomposition of tar (with or without steam) over the carbon-based catalyst probably performed via the condensation/polymerization to generate coke over the porous surface of the catalyst and the form coke subsequently react with steam (external steam or pyrolytic steam) to generate gaseous product [13, 24].

Table 12 Physical properties of the char samples after experiment

Spent char sample	Surface Properties		
	Average BET surface area ($m^2 g^{-1}$)	Total pore volume ($m^3 g^{-1}$)	Average pore size (A^o)
RS feeding			
CC600	236.7	0.226	38.2
CC700	242.9	0.240	39.5
CC800	270.5	0.265	39.1
C/RS600	257.2	0.201	31.3
C/RS700	320.0	0.246	30.7
C/RS800	301.3	0.236	31.3
RSC600	260.1	0.188	28.9
RSC700	320.2	0.201	29.7
RSC800	234.3	0.171	29.3
LN feeding			
CC600	243.9	0.237	38.8
CC700	259.9	0.252	38.8
CC800	298.0	0.293	39.4
C/LN600	305.4	0.261	34.1
C/LN700	375.6	0.322	34.3
C/LN800	395.7	0.334	33.7
LNC600	518.3	0.365	28.1
LNC700	524.9	0.376	28.6
LNC800	483.1	0.334	27.6

Fig 23 presents the SEM images of the spent catalysts. It was clearly observed that the surfaces of all spent catalysts were covered by the carbon particles (point C.) with round-smooth shapes, especially biomass pure chars i.e. RSC and LNC. It was also found the porous structure in cases of the spent coal/biomass blend chars (written as the dash-circle). This was clearly seen that coal/biomass blend chars could better prevent the carbon deposition during the tar steam reforming than that of the pure biomass chars. Hosokai et al. [24] reported that the way to maintain the catalytic activity of the char is to promote the steam reforming of the coke (generated from volatiles) by the AAEMs of the char. Consider in the effect of pyrolysis temperature, it was observed

that almost spent catalysts using in the steam reforming of tar released at 700ºC, except C/LN, had the highest BET surface area and total pore volume. It indicates that all catalysts could perform the best catalytic activity for steam reforming of tar that generated from the pyrolysis at 700ºC. This result was consistent with the carbon conversion as reported in Fig. 22. It could explain that the tar released at 700ºC which consisting of the mixture of oxygenated compounds, phenolic compounds and single-ring aromatic compounds, dominantly adsorb on the high porous surfaces of char then generate solid carbon called “coke”. The coke would react with steam with the catalytic function of the AAEM on the char to accelerate the steam reforming of carbon to produce more gaseous products. While, the tar released at 800ºC contains a lot of 2- or 3- rings aromatic hydrocarbons could condense on the char surfaces to generate coke but the form coke would more stable due to the high aromatic molecules that more difficult to decompose into the gas products.

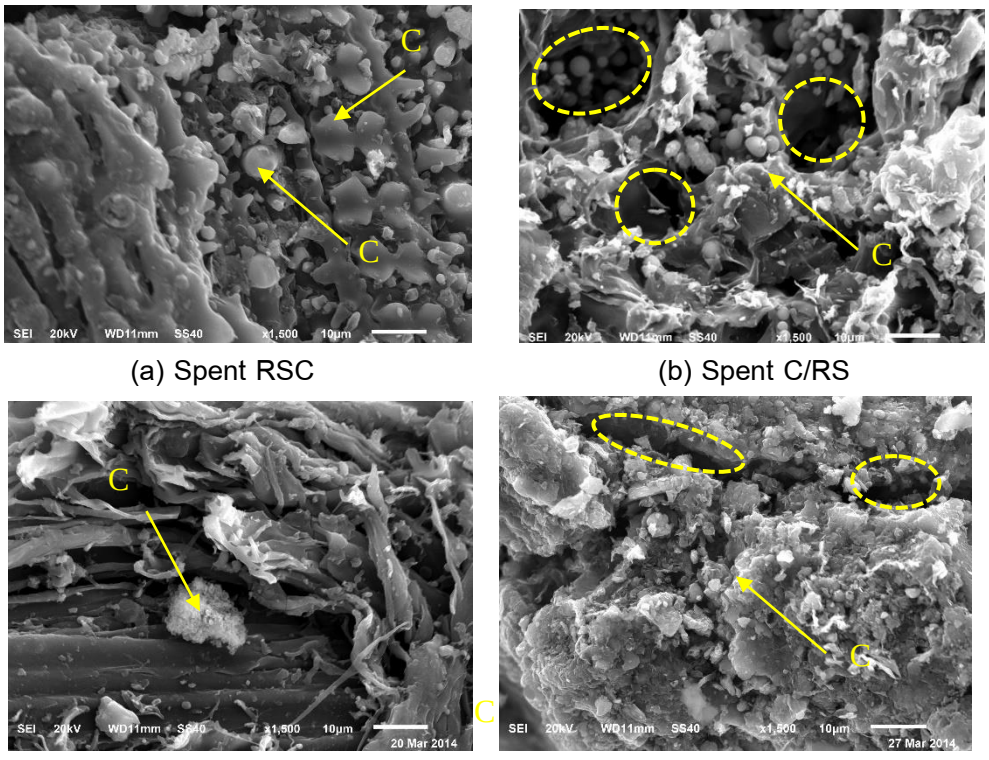

(a) Spent RSC (b) Spent C/RS

(c) Spent LNC (d) Spent C/LN

Fig. 23 SEM images of the spent catalysts after tar steam reforming

In the view point of catalyst type, it was found that coal/biomass blended char (both C/RS and C/LN) showed the better catalytic performance in terms of the higher carbon conversion into gas and lower carbon conversion into tar than that of the pure

biomass char (RSC and LNC) for all pyrolysis temperature. This result agrees with the previous our study [21]. It could explain by the enhancement of char surface properties obtained from the co-pyrolysis of coal and biomass. AAEM formation on the char surface was also the important parameter reflecting on the catalytic performance of the char. In cases of C/RS and C/LN, AAEM, in particular K, could be formed in K-Silicates due to the relatively low K/Si molar ratio. While, in cases of RSC and LNC, the K may be formed as the K-O-C or phenolate group on the char surfaces. The higher thermal stability of the K-silicates than those of phenolate groups may be the main key to maintain the catalytic activity for tar steam reforming of the C/LN and C/RS char. This result is consistent with the previously study [21].

Effect of devolatilization temperature on the catalytic tar steam reforming in term of gas production yield is presented in Fig. 24. Note that gas production presented here was the net gas production generating from the steam reforming of biomass derived tar after subtracting the gas generation from the char itself. It was found that with the presence of catalyst H_2, CO and CO_2 increased significantly both in cases of tar steam reforming of rice straw and LN wood. During the tar steam reforming, coke might generated over the catalyst surfaces and then gasified with steam to generate the higher H_2, CO and CO_2 production via coke steam reforming and hydrocarbon steam reforming as expressed in Eq. (11) – (12). In addition, the presence of AAEM species such as K on the catalyst surface would promote the water-gas shift reaction to produce higher CO_2 and H_2 as expressed in Eq. (13).

Coke steam reforming

$$C\ (\text{form coke}) + H_2O \longleftrightarrow H_2 + CO_2 + CO \text{ and hydrocarbons} \quad (11)$$

Hydrocarbon reforming

$$C_xH_y + H_2O \longleftrightarrow H_2 + CO_2 + CO \quad (12)$$

Water-gas Shift

$$CO + H_2O \longleftrightarrow CO_2 + H_2 \quad (13)$$

Consider the effect of devolatilization temperature, with the presence of catalyst, total gas yield was achieved the highest value at devolatilization temperature of 700ºC for all catalysts. At the devolatilization temperature of 700ºC, H_2 and CO_2 were higher than that the pyrolysis temperature of 600 and 800ºC. It was due to the different tar composition of biomass released from 700 ºC and the other 600 and 800 ºC.

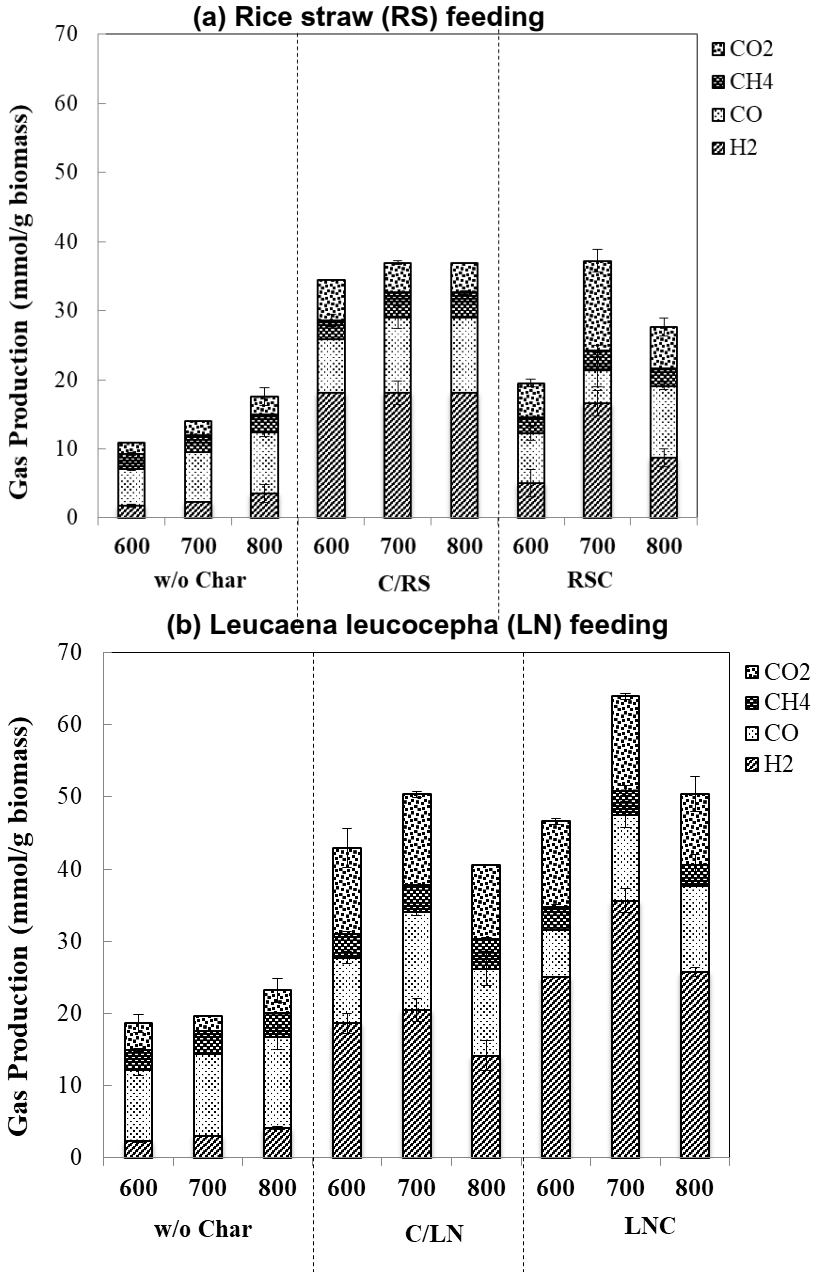

Fig. 24 Catalytic steam reforming of biomass derived tar (a) rice straw and (b) Leucaena leucocepha (LN) in terms of carbon conversion

Biomass tar both RS and LN tar released at pyrolysis temperature of 700 ºC mainly consists of phenolic compounds and 1-ring aromatic derivatives such as methylbenzene. These compounds was less stable than that of the tar released from 800 ºC which may contain the high amount of PAHs. It was speculated that the coke generated from the volatiles released from the pyrolysis at 700ºC dominantly reacted with steam via coke steam reforming subsequence hydrocarbon steam reforming following Eq. (11)-(12). At pyrolysis temperature of 700 ºC, the presence of pure biomass char dominantly gave the higher in H_2 and CO_2 when comparing with the

presence of coal/biomass blended chars. It was probably due to presence of K in phenolate form which was more reactive sites for water-gas shift reaction (Eq. (13)) than that of the K in silicate forms [25]. In the view point of biomass tar, it was found that the gas production from steam reforming of LN was significantly higher than that the steam reforming of RS, especially at the pyrolysis temperature at 700 ºC. It was probably due to the different tar composition between RS and LN tars. At devolatilization temperature of 700ºC, RS mainly comprise of 2-methlyphenol, while the major component of LN tar was phenol. It could be stated that phenol has the symmetric structure and compatible to absorb on the catalyst surface more than the 2-methylphenol.

4.3 Conclusion

In this study, the decomposition of biomass derived tar over the pyrolyzed char was carried out in a two-stage fixed bed reactor. Rice straw (RS) and Leucaena wood (LN) were selected as the biomass sample. Effect of devolatilization temperature on tar composition was investigated. Moreover, the effects of char type and tar composition on the catalytic tar decomposition in both thermal cracking and steam reforming were studied. Five types of char were prepared, i.e. coal char (CC), coal/RS blended char (C/RS), rice straw char (RSC), coal/LN blended char (C/LN) and LN char (LNC). Results showed that tar conversion and gas production increased drastically with the presence of all chars, especially with the addition of steam. It can be stated that all chars could act as the catalyst for biomass derived tar decomposition. At the same devolatilization temperature, blended char, both C/RS and C/LN, performed a better catalytic performance for tar thermal cracking than that of pure biomass char but comparable to the CC. The enhancement of BET surface area of the C/RS and C/LN during co-pyrolysis is the main key to achieve the higher catalytic activity. However, with the external steam, the catalytic activity of the blend char was less dominant than that of CC due to the promotion of AAEM volatilization by steam. Consider the effect of devolatilization temperature, it revealed that biomass tar released at 700 ºC could be highly cracked over all the prepared chars. It was due to at 700ºC tar was composed of the mixture between phenolic compounds and single ring-aromatic derivatives which might be easier cracked than that the polyaromatic hydrocarbons (PAHs) presenting in the tar released at 800ºC. For C/RS and RSC, the main mechanism for tar conversion is about the potentially deposition of oxygenated hydrocarbons on the char as well as the catalytic role of AAEMs (i.e. K) to promote the coke steam gasification. While the

mechanism of CC was the dominant tar deposition, in particular aromatic compounds and the supporting coke gasification by the inherent high Ca content. Therefore, this study emphasized the possibility of tar removal process in biomass gasification by using the low-cost carbon based catalyst.

4.4 Output and publications

International Journal

Suwat Mueangta, Prapan Kuchothara and Supachita Krerkkaiwan. “Effect of pyrolysis temperature on catalytic steam reforming of biomass derived tar over the coal/biomass blended char in a Two-Stage fixed bed reactor” (in preparation)

International Conference

Suwat Mueangta, Prapan Kuchothara and Supachita Krerkkaiwan. “Decomposition of Rice Straw derived Tar over the Co-pyrolysis Char in a Two-Stage fixed bed reactor” Oral presentation in **2018 International Conference on Engineering, Technology, and Applied Science – Summer Session (ICETA-Summer 2018), August 17-19, Sapporo, Hokkaido, Japan**

Reference

[1] D.C. Elliott, Relation of Reaction Time and Temperature to Chemical Composition of Pyrolysis Oils, in: Pyrolysis Oils from Biomass, American Chemical Society, 1988, pp. 55-65.

[2] C. Li, K. Suzuki, Tar property, analysis, reforming mechanism and model for biomass gasification—An overview, Renewable and Sustainable Energy Reviews, 13 (2009) 594-604.

[3] J. Wannapeera, X. Li, N. Worasuwannarak, R. Ashida, K. Miura, Production of High-Grade Carbonaceous Materials and Fuel Having Similar Chemical and Physical Properties from Various Types of Biomass by Degradative Solvent Extraction, Energy & Fuels, 26 (2012) 4521-4531.

[4] Y. Zhao, D. Feng, Y. Zhang, Y. Huang, S. Sun, Effect of pyrolysis temperature on char structure and chemical speciation of alkali and alkaline earth metallic species in biochar, Fuel Processing Technology, 141, Part 1 (2016) 54-60.

[5] K. Yip, F. Tian, J.-i. Hayashi, H. Wu, Effect of Alkali and Alkaline Earth Metallic Species on Biochar Reactivity and Syngas Compositions during Steam Gasification, Energy & Fuels, 24 (2010) 173-181.

[6] D.M. Keown, G. Favas, J.-i. Hayashi, C.-Z. Li, Volatilisation of alkali and alkaline earth metallic species during the pyrolysis of biomass: differences between sugar cane bagasse and cane trash, Bioresource Technology, 96 (2005) 1570-1577.

[7] E. Schröder, K. Thomauske, C. Weber, A. Hornung, V. Tumiatti, Experiments on the generation of activated carbon from biomass, Journal of Analytical and Applied Pyrolysis, 79 (2007) 106-111.

[8] M. Fan, W. Marshall, D. Daugaard, R.C. Brown, Steam activation of chars produced from oat hulls and corn stover, Bioresource technology, 93 (2004) 103-107.

[9] P. Fu, S. Hu, J. Xiang, L. Sun, S. Su, J. Wang, Evaluation of the porous structure development of chars from pyrolysis of rice straw: Effects of pyrolysis temperature and heating rate, Journal of Analytical and Applied Pyrolysis, 98 (2012) 177-183.

[10] E.P. Barrett, L.G. Joyner, P.P. Halenda, The Determination of Pore Volume and Area Distributions in Porous Substances. I. Computations from Nitrogen Isotherms, Journal of the American Chemical Society, 73 (1951) 373-380.

[11] D.P. Serrano, J.A. Botas, J.L.G. Fierro, R. Guil-López, P. Pizarro, G. Gómez, Hydrogen production by methane decomposition: Origin of the catalytic activity of carbon materials, Fuel, 89 (2010) 1241-1248.

[12] N.B. Klinghoffer, M.J. Castaldi, A. Nzihou, Catalyst properties and catalytic performance of char from biomass gasification, Industrial & engineering chemistry research, 51 (2012) 13113-13122.

[13] Y.-l. Zhang, Y.-h. Luo, W.-g. Wu, S.-h. Zhao, Y.-f. Long, Heterogeneous Cracking Reaction of Tar over Biomass Char, Using Naphthalene as Model Biomass Tar, Energy & Fuels, 28 (2014) 3129-3137.

[14] K.S. Sing, Reporting physisorption data for gas/solid systems with special reference to the determination of surface area and porosity (Recommendations 1984), Pure and applied chemistry, 57 (1985) 603-619.

[15] J.F. González, S. Román, J.M. Encinar, G. Martínez, Pyrolysis of various biomass residues and char utilization for the production of activated carbons, Journal of Analytical and Applied Pyrolysis, 85 (2009) 134-141.

[16] S. Hosokai, K. Norinaga, T. Kimura, M. Nakano, C.-Z. Li, J.-i. Hayashi, Reforming of Volatiles from the Biomass Pyrolysis over Charcoal in a Sequence of Coke

Deposition and Steam Gasification of Coke, Energy & Fuels, 25 (2011) 5387-5393.

[17] S. Krerkkaiwan, A. Tsutsumi, P. Kuchonthara, Biomass derived tar decomposition over coal char bed, ScienceAsia, 39 (2013) 511-519.

[18] N.B. Klinghoffer, M.J. Castaldi, A. Nzihou, Influence of char composition and inorganics on catalytic activity of char from biomass gasification, Fuel, 157 (2015) 37-47.

[19] A. Zolin, A. Jensen, P.A. Jensen, F. Frandsen, K. Dam-Johansen, The Influence of Inorganic Materials on the Thermal Deactivation of Fuel Chars, Energy & Fuels, 15 (2001) 1110-1122.

[20] S. Krerkkaiwan, C. Fushimi, A. Tsutsumi, P. Kuchonthara, Synergetic effect during co-pyrolysis/gasification of biomass and sub-bituminous coal, Fuel Processing Technology, 115 (2013) 11-18.

[21] S. Krerkkaiwan, S. Mueangta, P. Thammarat, L. Jaisat, P. Kuchonthara, Catalytic Biomass-Derived Tar Decomposition Using Char from the Co-pyrolysis of Coal and Giant Leucaena Wood Biomass, Energy & Fuels, 29 (2015) 3119-3126.

[22] H. Wu, D.M. Quyn, C.-Z. Li, Volatilisation and catalytic effects of alkali and alkaline earth metallic species during the pyrolysis and gasification of Victorian brown coal. Part III. The importance of the interactions between volatiles and char at high temperature, Fuel, 81 (2002) 1033-1039.

[23] F. Nestler, L. Burhenne, M.J. Amtenbrink, T. Aicher, Catalytic decomposition of biomass tars: The impact of wood char surface characteristics on the catalytic performance for naphthalene removal, Fuel Processing Technology, 145 (2016) 31-41.

[24] S. Hosokai, K. Kumabe, M. Ohshita, K. Norinaga, C.-Z. Li, J.-i. Hayashi, Mechanism of decomposition of aromatics over charcoal and necessary condition for maintaining its activity, Fuel, 87 (2008) 2914-2922.

[25] C. Fushimi, T. Wada, A. Tsutsumi, Inhibition of steam gasification of biomass char by hydrogen and tar, Biomass and Bioenergy, 35 (2011) 179-185.

Output จากโครงการวิจัยที่ได้รับทุนจาก สกว.

1. ผลงานตีพิมพ์ในวารสารวิชาการนานาชาติ (ระบุชื่อผู้แต่ง ชื่อเรื่อง ชื่อวารสาร ปี เล่มที่ เลขที่ และหน้า) หรือผลงานตามที่คาดไว้ในสัญญาโครงการ

   1.1) Supachita Krerkkaiwan and Suneerat Fukuda. “Catalytic effect of Rice Straw derived Chars on the Decomposition of Naphthalene: Influence of steam activation and solvent treatment during char preparation” **(in preparation)**

   1.2) Suwat Mueangta, Prapan Kuchothara and Supachita Krerkkaiwan. “Effect of pyrolysis temperature on catalytic steam reforming of biomass derived tar over the coal/biomass blended char in a Two-Stage fixed bed reactor” **(in preparation)**

2. การนำผลงานวิจัยไปใช้ประโยชน์
   - เชิงพาณิชย์ (มีการนำไปผลิต/ขาย/ก่อให้เกิดรายได้ หรือมีการนำไปประยุกต์ใช้โดยภาคธุรกิจ/บุคคลทั่วไป)
   - เชิงนโยบาย (มีการกำหนดนโยบายอิงงานวิจัย/เกิดมาตรการใหม่/เปลี่ยนแปลงระเบียบข้อบังคับหรือวิธีทำงาน)
   - เชิงสาธารณะ (มีเครือข่ายความร่วมมือ/สร้างกระแสความสนใจในวงกว้าง)
   - **เชิงวิชาการ (มีการพัฒนาการเรียนการสอน/สร้างนักวิจัยใหม่)** องค์ความรู้ที่ได้จากงานวิจัยนี้ สามารถนำไปต่อยอดใช้ได้จริงในอุตสาหกรรม โดยเฉพาะอย่างยิ่งในกระบวนการผลิตแก๊สสังเคราะห์จากชีวมวล โดยใช้ตัวเร่งปฏิกิริยาที่มีราคาถูกและมีประสิทธิภาพในการกำจัดทาร์สูง ได้อย่างเหมาะสม
3. อื่นๆ (เช่น ผลงานตีพิมพ์ในวารสารวิชาการในประเทศ การเสนอผลงานในที่ประชุมวิชาการ หนังสือ การจดสิทธิบัตร)

   3.1) Supachita Krerkkaiwan and Suneerat Fukuda. “Decomposition of Naphthalene over Rice straw derived carbon-based catalysts: Influence of steam and solvent during catalyst preparation” Poster presentation in **TRF-OHEC Annual Congress 2017 (TOAC2017)** which held in The Regent Beach Cha-am, Petchaburi, during 11- 13 January 2017**.**

   3.2) Suwat Mueangta, Prapan Kuchothara and Supachita Krerkkaiwan. “Decomposition of Rice Straw derived Tar over the Co-pyrolysis Char in

a Two-Stage fixed bed reactor" Oral presentation in **2018 International Conference on Engineering, Technology, and Applied Science – Summer Session (ICETA-Summer 2018),** August 17-19, Sapporo, Hokkaido, Japan.